

CLUSTERING, NETWORK CODING AND COVERAGE
MAXIMIZATION IN COGNITIVE RADIO SENSOR NETWORKS

by

Mustafa Özger

A Thesis Submitted to the
Graduate School of Engineering
in Partial Fulfillment of the Requirements for
the Degree of

Master of Science

in

Electrical and Electronics Engineering

Koç University

September 5, 2013

Koç University
Graduate School of Sciences and Engineering

This is to certify that I have examined this copy of a master's thesis by

Mustafa Özger

and have found that it is complete and satisfactory in all respects,
and that any and all revisions required by the final
examining committee have been made.

Committee Members:

Özgür B. Akan, Ph. D. (Advisor)

A. Murat Tekalp, Ph. D.

Öznur Özkasap, Ph. D.

Date:

*Anneme ve Babama,
Fatma ve Ahmet Özger.*

ABSTRACT

The spectrum scarcity challenge is a natural consequence of increasing demand for wireless communication. This situation has triggered the use of opportunistic spectrum access schemes in wireless communications. The key technology addressing this challenge and enabling opportunistic spectrum access is cognitive radio. Wireless sensor network (WSN) suffers from the spectrum scarcity problem due to the fixed frequency assignment policy. Cognitive radio stands as a promising solution to this problem in WSNs. Wireless sensor nodes with cognitive radio capability can access different spectrum bands dynamically. This defines a new sensor networking paradigm, i.e., Cognitive Radio Sensor Networks (CRSN). The unique characteristics of CRSN necessitates energy-efficient and spectrum-aware solutions. In this thesis, we first propose a spectrum-aware clustering protocol for CRSN. We form non-isolated clusters between event and sink in accordance with event-driven communication nature. Simulation results show that our protocol is more energy-efficient than other protocols in literature. Next, we investigate the effect of network coding in CRSN. Network Coding is a novel technique enabling encoding operation instead of store-and-forward approach. The advantages and disadvantages of using network coding are presented. Finally, we consider wireless networked control system consisting of separate cognitive radio sensor subnetworks. The system state is estimated using Kalman filter. We find critical packet arrival probability for bounded expected state estimation covariance and obtain the maximum total coverage area of CRSN with maximum cost-efficiency.

ÖZETÇE

Tayf kıtlığı sorunu kablosuz haberleşme için artan talebin doğal sonucudur. Bu durum kablosuz haberleşmede fırsatçı tayf erişim kullanımını tetiklemiştir. Bu zorluğun üstesinden gelen ve fırsatçı tayf erişimine olanak sağlayan anahtar teknoloji bilişsel radyodur. Kablosuz algılayıcı ağlar (WSN) da sabit tayf atama prensibi nedeniyle tayf kıtlığı probleminden zarar görmektedir. Bilişsel radyo kabiliyetli kablosuz algılayıcı düğümleri değişik tayf bantlarına dinamik olarak erişir. Bu, ismi bilişsel radyo algılayıcı ağlar (CRSN) olan, yeni bir ağ paradigmasını tanımlar. Bilişsel radyo algılayıcı ağların benzersiz özellikleri enerji-verimli ve tayf-bilinçli çözümleri gerektirmiştir. Bu tezde ilk olarak tayf-bilinçli kümeleme protokolü önerilmiştir. Bilişsel radyo algılayıcı ağların (CRSN) olaygüdümlü haberleşme doğasına uygun olarak olay ile alıcı düğümü arasında birbirinden izole olmayan kümeler oluşturulmuştur. Benzetim sonuçları yöntemimizin bu alandaki diğer yöntemlerden enerji açısından daha verimli olduğunu göstermiştir. Sonrasında, bilişsel radyo algılayıcı ağlarında ağ kodlamasının etkileri incelenmiştir. Depola-ve-yolla yaklaşımı yerine kodlama işlemine olanak sağlayan ağ kodlaması özgün bir tekniktir. Ağ kodlamasının faydaları ve zararları sunulmuştur. Son olarak ayrık bilişsel radyo algılayıcı sensor alt ağlarından oluşan kablosuz ağı kontrol sistemlerine bakılmıştır. Sistem durumu Kalman süzgeci aracılığıyla tahmin edilmektedir. Beklenen durum tahmininin ortak değişintisinin sınırlı olması için gereken kritik paket geliş olasılığı ve azami maliyet uygunluğu ile azami toplam kapsama alanı bulunmuştur.

ACKNOWLEDGMENTS

I would like to gratefully acknowledge the enthusiastic supervision of Dr. Özgür B. Akan in all steps of the development of this work. He taught me not just how to conduct research, but how to achieve success in life. I achieved more than I ever dreamed of in two years by his guidance and help, and I am proud of being one of his students.

I would like to thank to Dr. A. Murat Tekalp and Dr. Öznur Özkasap for taking part in my thesis committee and for their invaluable suggestions and comments.

I want to thank the Next-generation and Wireless Communications Laboratory members due to their friendship and collaboration during last two years.

I want to acknowledge the support of TÜBİTAK and Koç University, which made the completion of this thesis possible.

I thank my parents, Fatma and Ahmet, and my sister Zehra for believing in me and trusting me at every step I have taken so far. I am very lucky to be a part of such a wonderful family.

TABLE OF CONTENTS

Abstract	iv
Özetçe	v
Acknowledgments	vi
List of Tables	x
List of Figures	xi
Abbreviations	xiii
Chapter 1: Introduction	1
1.1 Cognitive Radio Sensor Networks	1
1.2 Spectrum-aware Clustering in Cognitive Radio Sensor Networks	3
1.3 Network Coding in Cognitive Radio Sensor Networks	4
1.4 Coverage Maximization in Cognitive Radio Enabled Wireless Networked Controlled Systems	5
1.5 Research Objectives and Solutions	6
1.5.1 Event-to-Sink Coordination in Cognitive Radio Sensor Networks	6
1.5.2 On the Effects of Network Coding in Cognitive Radio Sensor Networks	6
1.5.3 On the Maximum Coverage Area of Cognitive Radio Enabled Wireless Networked Control Systems with Maximum Cost-Efficiency under Stability Constraint	7
1.6 Thesis Outline	7

Chapter 2:	Event-to-Sink Coordination in Cognitive Radio Sensor Networks	9
2.1	Introduction	9
2.2	Related Work	12
2.3	Network Model	13
2.3.1	Cognitive Radio Model	13
2.3.2	Primary Channel Usage Model	15
2.4	Event-driven Spectrum-Aware Clustering (ESAC)	17
2.4.1	Determination of Eligible Nodes For Clustering	17
2.4.2	Clustering Algorithm	20
2.4.3	Control overheads of ESAC	25
2.5	On the Re-clustering Probability of a Cluster	25
2.6	Performance Evaluation	28
2.6.1	Ratio of eligible nodes in the network	28
2.6.2	Delay, Energy and Connectivity	31
Chapter 3:	On the Effects of Network Coding in Cognitive Radio Sensor Networks	37
3.1	Introduction	37
3.2	System Model	40
3.2.1	Network Model	40
3.2.2	Traffic Model	40
3.3	Network Coding	41
3.3.1	Practical Network Coding	42
3.4	Performance Evaluation	43
3.4.1	Simulation Environment	44
3.4.2	Energy-Efficiency	44
3.4.3	Packet delivery ratio	47
Chapter 4:	On the Maximum Coverage Area of Wireless Networked Control Systems with Maximum Cost-Efficiency under Stability Constraint	48

4.1	Introduction	48
4.2	Kalman Filtering with Partial Observation Losses	51
4.3	Multi-Hop Wireless Ad-Hoc Sensor Network Models and Connectivity	55
4.3.1	Homogeneous Network Model	55
4.3.2	Heterogeneous Network Model	57
4.4	Maximum Coverage Area of Cost-Efficient Networks Under Stability Constraint	59
4.5	Numerical Analysis	62
4.5.1	Optimum Hop-Diameter of Subnetworks	63
4.5.2	Maximum Total Coverage Area of Homogeneous Network	64
4.5.3	Maximum Total Coverage Area of Heterogeneous Network	66
Chapter 5:	Conclusions and Future Research Directions	69
5.1	Research Contributions	69
5.1.1	Event-to-Sink Coordination in Cognitive Radio Sensor Networks	69
5.1.2	On the Effects of Network Coding in Cognitive Radio Sensor Networks	70
5.1.3	On the Maximum Coverage Area of Wireless Networked Control Systems with Maximum Cost-Efficiency under Stability Constraint	70
5.2	Future Research Directions	71
	References	72
	Curriculum Vitae	80

LIST OF TABLES

2.1	Notations For Clustering Protocol	16
2.2	Iterations for Cluster-head node 1 in Fig. 2.4	24

LIST OF FIGURES

1.1	A typical CRSN topology.	2
2.1	Typical CRSN topology with event and sink.	14
2.2	Semi-Markov model for channel c	17
2.3	Illustration of an eligibility scenario.	18
2.4	One-hop and two-hop neighbors of cluster-head node 1 and its constructed tree. . .	23
2.5	Fraction of eligible nodes in the network vs. D_{es} for different R (m) when $r = 20$ m and $N = 200$	29
2.6	Fraction of eligible nodes in the network vs. D_{es} for different N when $r = 20$ m and $R = 30$ m.	30
2.7	Fraction of eligible nodes in the network vs. D_{es} for different r (m) when $R = 20$ m and $N = 200$	31
2.8	T_{cls} (msec) vs. D_{es} (m) for different R (m) when $r = 20$ m and $N = 200$	32
2.9	T_{cls} (msec) vs. D_{es} (m) for different N when $R = 30$ m and $r = 20$ m.	32
2.10	T_{cls} (msec) vs. D_{es} (m) for different r (m) when $R = 20$ m and $N = 200$	33
2.11	E_c (mJ) vs. D_{es} (m) for different R (m) when $r = 20$ m and $N = 100$	33
2.12	E_c (mJ) vs. D_{es} (m) for different N when $R = 20$ m and $r = 20$ m.	34
2.13	E_c (mJ) vs. D_{es} (m) for different r (m) when $R = 20$ m and $N = 200$	35
2.14	Average energy consumed per node(μ J) vs. R (m) ($N = 200$ and $r = 15$ m)	35
2.15	Average connectivity per cluster vs. r (m) ($N = 200$ and $R = 20$ m)	36
3.1	Abstraction of a sensor network scenario where multiple nodes send packets to the sink.	39
3.2	Total energy consumption (mJ) with respect to r (m) with and without network coding. . .	45

3.3	Total energy consumption (mJ) with respect to R (m) with and without network coding.	45
3.4	Total energy consumption (mJ) with respect to respect to D_{es} (m) with and without network coding.	46
3.5	Packet delivery ratio per event with respect to transmission range.	47
4.1	The block diagram of the WCSN.	52
4.2	The model of the homogeneous multi-hop wireless ad-hoc subnetworks.	56
4.3	The model of the heterogeneous multi-hop wireless ad-hoc subnetworks.	57
4.4	d_i^{opt} (a) with respect to N for different β values and (b) with respect to α for different N values.	63
4.5	S^T with respect to (a) r_0 for different β values, (b) N for different β values, and (c) α for different N values.	65
4.6	S_T^{ht} with respect to (a) r_s for different β values, (b) r_p for different β values, (c) α for different N values, and (d) Π_1 for different N values.	67

ABBREVIATIONS

WSN	Wireless Sensor Networks
CRSN	Cognitive Radio Sensor Networks
CR	Cognitive Radio
CRN	Cognitive Radio Network
DSA	Dynamic Spectrum Access
OSA	Opportunistic Spectrum Access
ESAC	Event-driven Spectrum-Aware Clustering
SOC	Spectrum Opportunity Clustering
CH	Cluster-head
ESDC	Event to Sink Directed Clustering
SU	Secondary User
PU	Primary user
EFC_REQ	Eligibility for Clustering Request
EFC_REP	Eligibility for Clustering Reply
C_REQ	Clustering Request
C_REP	Clustering Reply
NC	Network Coding
LNC	Linear Network Coding
RLNC	Random Linear Network Coding
NCS	Networked Control System
WNCS	Wireless Networked Control System
MIMO	Multiple Input Multiple Output

Chapter 1

INTRODUCTION

The proliferation of wireless communication devices causes congestion in electromagnetic spectrum [1]. The spectrum resource is scarce, and it is underutilized by the fixed frequency assignment policies. Cognitive radio has become a promising solution to the inefficient utilization and the scarcity of spectrum resource [2]. Cognitive cycle operations enable opportunistic spectrum access which increases communication quality and improves channel utilization [3]. These unique features of cognitive radio overcome the challenges posed by fixed spectrum assignment policies. Cognitive radio sensor networks (CRSN) is a solution for spectrum scarcity problem in wireless sensor networks (WSN) [4]. CRSN nodes detect available channels by spectrum sensing, and determine communication channel by spectrum decision, and change their operation frequencies by spectrum hand-off if primary users appear on the communication channel. CRSN is an event-based system such that events trigger the communication. Event readings of the sensors collaboratively conveyed in multi-hop manner from event to sink. Despite improvements in spectrum utilization by DSA capability, energy-efficient solutions for CRSN are required due to resource-constrained nature of CRSN inherited from WSN.

1.1 Cognitive Radio Sensor Networks

Fixed frequency assignment approach of WSN suffers from the spectrum scarcity problem. Cognitive radio technology is enabled in wireless sensor nodes to eliminate this problem. This fact reveals a new sensor network paradigm, i.e., cognitive radio sensor networks [4]. CRSN nodes is provided with dynamic spectrum access (DSA) capability to utilize different spectrum bands. They use cognitive cycle operations for opportunistic spectrum access (OSA).

A typical topology formed by CRSN nodes is shown in Fig. 1.1. Primary and secondary net-

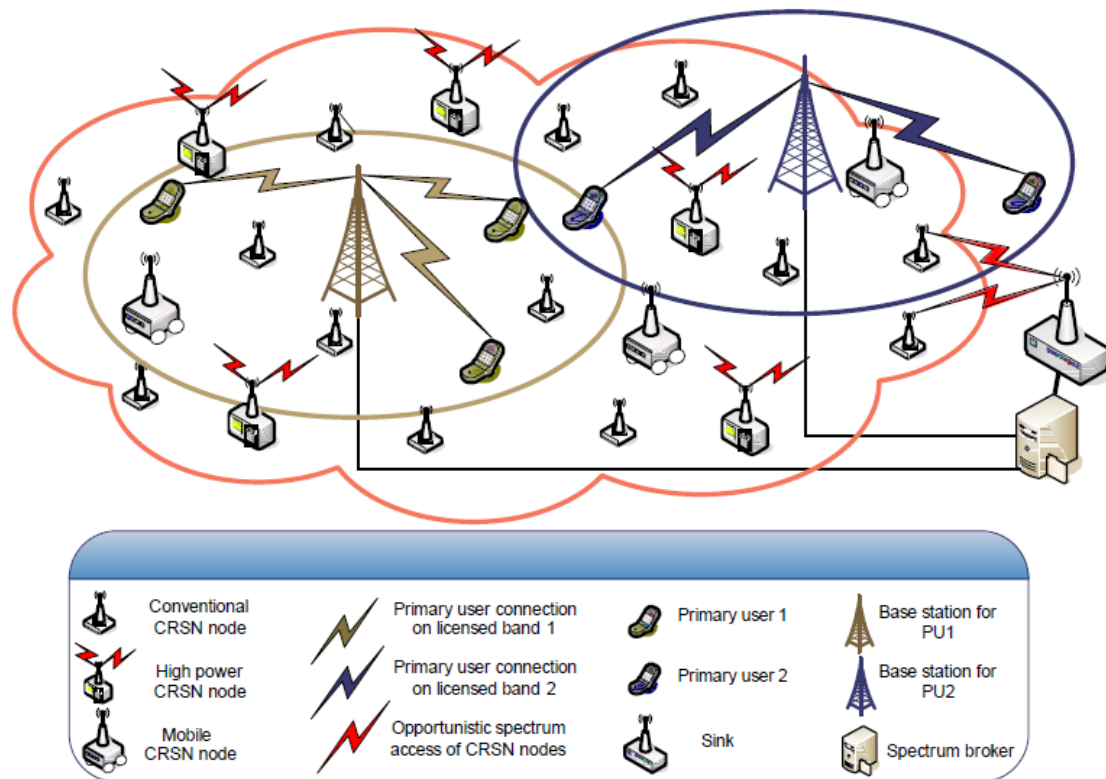


Figure 1.1: A typical CRSN topology.

work coexist in this topology. Primary network users are legacy user that they operate on the licensed channels without any permission. Secondary network users are CRSN nodes which perform sensing on the environments. They communicate with each other on licensed bands opportunistically without any interference to the primary network.

In this thesis, we study the challenges posed by cognitive radio sensor networks. We first propose an event-driven spectrum-aware clustering protocol for CRSN. The formed clusters are non-isolated. The clusters are between event and sink in accordance with event-driven communication nature. Next, we investigate the effect of network coding in CRSN. Network Coding is being used as a novel technique in centralized and distributed wireless networks. It enables encoding operation instead of store-and-forward approach. The advantages and disadvantages of using network coding are presented. Finally, we consider wireless networked control system consisting of separate cognitive

radio sensor subnetworks. The system state is estimated using Kalman filter. We find critical packet arrival probability for bounded expected state estimation covariance and obtain the maximum total coverage area of CRSN with maximum cost-efficiency.

1.2 Spectrum-aware Clustering in Cognitive Radio Sensor Networks

Inefficient spectrum utilization of traditional fixed spectrum assignment approach has triggered the use of dynamic spectrum access (DSA) schemes in wireless communications. Communication technology enabling DSA is cognitive radio (CR) [3]. Cognitive radios have the capability to sense spectrum bands in order to detect empty spectrum portions. With this capability, CRs can utilize spectrum vacancies opportunistically by changing their operating parameters [2]. Hence, the opportunistic spectrum access (OSA) capability overcomes the spectrum scarcity challenge and increases spectrum utilization efficiency.

Wireless sensor nodes equipped with cognitive radio has revealed a new network paradigm which is called cognitive radio sensor networks (CRSN) [4]. Sensor nodes can benefit from the advantages of DSA so that they can communicate intermittently over the licensed bands which is owned by primary users. A CRSN node determines available channels by spectrum sensing and the communication channel by spectrum decision and changes its operation frequency by spectrum hand-off if a primary user appears on that channel. By these functionalities, cognitive radios collaborate with neighbors in order to deliver event samples from event region to the sink in multi-hop manner in opportunistic radio environment.

In addition to addressing spectrum management challenges by CR capabilities, CRSN imposes energy and hardware limitation challenges inherited from WSN. The solutions for WSN do not consider CR functionalities and hence do not address CR challenges. On the other hand, the existing solutions for cognitive radio network do not take into account energy and hardware challenges. Even though there are extensive studies on WSN and CRN, CRSN has been receiving interest from the community lately. The recent existing works focus on channel management scheme [6], packet size optimization [8], and reliability and congestion control [7].

Clustering is one of the most important research issues of CRSN that is not investigated thoroughly. Clustering is a structured way to manage topology effectively and to facilitate spatial reuse

of resources to increase the system capacity [17]. There are several studies on clustering for wireless sensor networks and wireless ad-hoc networks [11, 12, 13, 14, 15, 16]. In these approaches, clustering divides ad-hoc network into self organized structures each managed by cluster-heads. Those act as a central entity in their corresponding cluster for the efficient and reliable data transmission. Clusters handle the communication in an organized manner by arranging inter-cluster and intra-cluster communication. In WSNs, cluster-heads are selected according to the node ID [19], residual energy [20] and weight of nodes [21]. These clustering studies do not address the dynamic spectrum access challenges hence they are not applicable in CRSN regime.

Clustering for cognitive radio networks requires additional constraint which is the condition of grouping nodes according to similar vacant bands in spatial neighborhood. This situation in clustering is termed as *spectrum-aware* clustering. Clustering in opportunistic spectrum access environment requires to take into account local variations of the licensed user activities [22, 23, 26, 27, 28, 29]. Clusters are valid if the nodes forming the cluster have at least one common channel. Dynamic spectrum access environment requires frequent re-clustering due to the variations of spectrum availabilities.

1.3 Network Coding in Cognitive Radio Sensor Networks

Network coding is a new technique pioneered by Alswede et al. [41]. It discards store-and-forward method in networks and enables the network nodes to make in-network processing. By this method, the nodes can make encoding operations and the messages generated by the source nodes can be encoded at the intermediate nodes and destination nodes can decode the source messages if enough number of encoded messages are received by the destination nodes. Li et al. [43] has showed that linear encoding operations are sufficient for achieving capacity of networks. Koetter and Medard [42] have revealed the algebraic approach for network coding in multicast networks. In [44], randomized network coding is investigated for multicast networks. Chou *et al.* have suggested network coding for practical networks by applying random network coding [57]. Furthermore, Koetter and Medard [42] have showed how to find the coefficients for linear encoding operation and the decodability at the destination nodes. By network coding, information packets do not flow as commodities, however, they can be mixed such that receivers can have coded packets to reconstruct

original messages.

Network coding makes it possible to achieve max-flow min-cut capacity for the multicast networks. This paradigm increases the network throughput. Nodes making encoding operations wait for the incoming links and take linear combinations of them for their output links. In the classical store-and-forward method, the incoming packets are destined to outgoing links immediately. Therefore, the channel is used every time if packets come. On the other hand, nodes listen for N packets and transmit one encoded packet instead. Intermediate nodes show less transmission efforts since they transmit only the encoded packets out of incoming packets. Less transmission effort is less energy consumption. This property is important for networks consisting of energy-constrained nodes. Furthermore, network coding is beneficial for avoiding adversary effects. The intruders do not interfere with the nodes easily since they should collect sufficient information to decode the necessary information. Due to these benefits, network coding can be used to overcome the challenges posed by different type of communication networks.

1.4 Coverage Maximization in Cognitive Radio Enabled Wireless Networked Controlled Systems

Cognitive radio sensor networks can be used in many applications. One of the most important application areas is wireless networked control system. The combination of communication and control systems is enabled by the developments on sensor systems. This integration revealed networked control systems (NCSs) where the communication system enables the sensor observation delivery [59, 60]. The control system components such as sensors, actuators and plants with wireless communication capabilities constitute a wireless networked control system (WNCS). The observations of the sensors deployed over a wide area are fed to the WNCS through a wireless network. The WNCSs have a wide application area such as smart grid, automatic management and navigation systems [61]. One fundamental problem in WNCSs is to have a wide coverage area.

The WNCS consists of cognitive radio sensor subnetwork. The output sensor measurements are transmitted over separate multi-hop cognitive radio sensor subnetworks. In these type of systems the observation process is divided into N parts and the system state is estimated using the Kalman filter. Furthermore, there is a critical arrival probability for a sensor measurement packet such that if

the packet arrival probability is larger than the critical value, it is guaranteed that the expected state estimation error covariance is bounded, and hence the WNCS is stable.

1.5 Research Objectives and Solutions

The objectives of our research and the solution approaches are explained in this section.

1.5.1 Event-to-Sink Coordination in Cognitive Radio Sensor Networks

Event delivery from event to sink requires coordination for communication between sensor nodes. Nodes can only communicate with each other if they are within transmission range and have at least a common channel. Vacant spectrum bands are locally and temporally correlated. In this thesis, our goal is to exploit this property by designating local coordinators in CRSN, and to offer spectrum coordination scheme by clustering. Clustering in such a highly dynamic radio environment requires frequent re-clustering and maintenance overheads. The gain by clustering can be mitigated by energy-consumption due to re-clustering and maintenance overheads. In this thesis, we present an event-driven spectrum-aware clustering protocol for CRSN. Overheads can be decreased by exploiting event-driven nature of CRSN. This decrease is achieved by forming clusters in the corridor between event region and sink after the detection of the event. We also form connected clusters in order to avoid isolated logical entities. We perform mathematical study to find average re-clustering probability of a cluster according to our network setup.

1.5.2 On the Effects of Network Coding in Cognitive Radio Sensor Networks

In this thesis, we investigate the response of CRSN in terms of energy and reliability while using network coding. Network coding is a well investigated technique for communication networks [41, 42, 43, 44]. It has been suggested to achieve max-flow capacity for multicast communication [41]. The network coding studies can be divided into theoretical [43, 44], simulation-based [53, 54] and implementation based [46] classes. None of these works studies the applicability of network coding in CRSN taking into account the challenges posed by cognitive radio capability and the resource-constraint of sensor network. Our approach relies on simulation-based study scrutinizing

the positive and negative effects of network coding and investigating the applicability of this novel technique in CRSN.

1.5.3 On the Maximum Coverage Area of Cognitive Radio Enabled Wireless Networked Control Systems with Maximum Cost-Efficiency under Stability Constraint

The integration of wireless communication and control systems revealed wireless networked control systems (WNCSs). One fundamental problem in WNCSs is to have a wide coverage area. For the first time in the literature, we address this problem and we obtain the maximum coverage area by solving an optimization problem. In this thesis, we consider a WNCS where the output sensor measurements are transmitted over separate multi-hop cognitive radio sensor subnetworks. We employ both homogeneous and cognitive radio multi-hop wireless sensor network models. The observation process is divided into N parts and the system state is estimated using the Kalman filter and we present the critical arrival probability for a sensor measurement packet such that if the packet arrival probability is larger than the critical value, it is guaranteed that the expected state estimation error covariance is bounded, and hence the WNCS is stable. We find the optimum hop-diameter of a multi-hop wireless ad-hoc subnetwork having maximum cost-efficiency under the constraint of the stability of the WNCS. Furthermore, under this constraint, we derive the maximum total coverage area of both the homogeneous and cognitive radio sensor wireless subnetworks with maximum cost-efficiency. The numerical analyses show that the maximum total coverage area can be increased by appropriately adjusting the number of sensors, the successful packet transmission probability between relay nodes, the transmission range of network nodes, and the eigenvalues of the system matrix.

1.6 Thesis Outline

This thesis is organized as follows. Chapter 2 presents our event-driven spectrum-aware clustering (ESAC) protocol. Next, we investigate our protocol in terms of energy-consumption, delay and connectivity. In Chapter 3, we investigate the effects of network coding in cognitive radio sensor networks. Simulation study is conducted to see the response of the network for different environments. In Chapter 5, we study the coverage maximization of wireless networked control systems

which consist of separate cognitive radio sensor subnetworks or wireless sensor subnetworks. The maximum coverage is found under the stability constraint with maximum cost-efficiency. Chapter 6 presents the research results with the discussion of the future issues.

Chapter 2

EVENT-TO-SINK COORDINATION IN COGNITIVE RADIO SENSOR NETWORKS

Cognitive radio capability and reconfigurability are solutions for spectrum scarcity problem in wireless sensor networks (WSN). CRSN is an event-based system such that events trigger the communication. Event readings of the sensors collaboratively conveyed in multi-hop manner from event to sink. The event detection causes bursty traffic in sensor networks. Hence, the communication after event detection requires coordination in opportunistic spectrum access (OSA) environment. In this chapter, we propose a spectrum-aware clustering protocol for event-to-sink coordination. It consists of two phases since the clusters are constructed from scratch upon the detection of an event. The first phase is the determination of nodes joining clustering, and the second one is to form clusters according to the spectrum availabilities among those nodes. Clusters are not preserved after the end of events. Furthermore, we obtained the probability of re-clustering for a cluster and studied how our approach decreases this probability. Performance evaluation shows that by means of event-to-sink approach only nodes between the event and the sink form cluster and consume energy for coordination. Our approach provides less energy consumption than whole network clustering approach. Furthermore, we investigate the extra delay occurs due to the spontaneous cluster formation.

2.1 Introduction

Fixed frequency allocation policies reveals the inefficient utilization of the electromagnetic spectrum. As wireless devices are becoming ubiquitous, the demand for spectrum use rises which causes spectrum scarcity problem. Despite this increase, spectrum is also inefficiently utilized both temporally and spatially according to FCC [1]. This problem has triggered the use of dynamic spectrum access (DSA) schemes in wireless communications. Wireless devices having DSA ability, called

cognitive radios (CRs), can perform cognitive cycle operations [3]. Hence, they can detect vacant spectrum bands and change their operating frequencies accordingly to enable opportunistic spectrum access [2]. This technology overcomes the spectrum scarcity challenge and increases spectrum utilization efficiency.

A new wireless network paradigm, namely cognitive radio sensor networks (CRSN), has been revealed by enabling opportunistic spectrum access (OSA) scheme on sensor nodes in wireless networks [4]. Apart from fixed frequency allocation approach in wireless sensor networks (WSN), sensor nodes opportunistically utilize licensed spectrum bands in CRSN. Cognitive radio sensor nodes sense spectrum to determine vacant bands, choose their operating frequencies by spectrum decision, and change the frequency by spectrum hand-off according to the licensed user activities. CRSN is a distributed network. Packets generated by event detecting nodes are transmitted in multi-hop manner from event region to sink in opportunistic spectrum environment without any central controller.

CRSN enhances the spectrum utilization of traditional sensor networks by its unique features. However, its realization imposes significant challenges due to the specific properties of cognitive radio and sensor networks, and the challenges are amplified by their unique union. Resource constraint is inherited from sensor networks. On the other hand, spectrum management is a result of cognitive radio capability of sensor nodes. The limited power capability requires energy-efficient and low cost solutions. Furthermore, dynamic radio environment due to the cognitive radio capability necessitates spectrum-awareness. However, WSN solutions are not spectrum-aware since they do not consider CR functionalities. On the other hand, cognitive radio network solutions discard hardware and energy limitations. There is a growing number of studies on CRSN to satisfy the requirements of cognitive radio and sensor network. Some of recent works focus on channel assignment according to residual energy [5], energy-efficient channel management scheme [6], packet size optimization [8], power and rate adaptation for maximization of information theoretical capacity [9] and performance analysis in terms of delay [10].

Clustering for ad hoc and sensor networks is well studied topic by research community [11, 12, 14, 16]. In [17], network is divided into logical structures according to some metrics in order to satisfy desired system requirements. Clustering is also proposed as an effective tool for resource

management and scalability in sensor networks [18]. This technique groups randomly deployed sensor nodes into clusters. Each one has a cluster-head which organizes inter-cluster and intra-cluster communication. Distributed wireless networks benefit from clustering to manage topologies with lifetime improvement, fault tolerance and load balancing.

Clustering has been applied to cognitive radio networks (CRN) recently [22, 23]. Clustering approaches in CRN differs from ones in WSN due to the spectrum heterogeneity. Clustering is considered as a tool for managing spectrum heterogeneity. In addition to spatial neighborhood for grouping, nodes are also clustered according to vacant spectrum bands. Each valid cluster has at least one common channel among its members. CRN nodes consider temporal and spatial variations of spectrum opportunities for the validity of clusters. Hence, this type of clustering approach termed as *spectrum-aware* clustering.

Clustering has not been investigated thoroughly for CRSN despite some efforts on cognitive radio networks (CRN). In our prior work [24], we propose a spectrum-aware clustering protocol for CRSN considering the event-driven communication nature. In this chapter, we investigate the effect of our proposed clustering approach in the reduction of re-clustering probability. We also propose our clustering scheme as an coordination tool between event-to-sink communication and obtain re-clustering probability according to our network model.

In a typical CRSN, event detecting nodes generate packets and they are transmitted collaboratively in multi-hop manner over available spectrum bands in CRSN. This requires coordination among nodes in such dynamic radio environment. Clustering is used as an energy-efficient spectrum coordination technique in order to deliver the event readings from event region to sink [24].

The communication pattern of CRSN needs event-to-sink coordination scheme. Furthermore, there are two constraints for the communication of two nodes in CRSN which are having at least one common channel and being within the transmission range. We exploit the spatially correlated spectrum bands for designating local coordinators in CRSN and offering spectrum coordination scheme by clustering. Clustering in such a highly dynamic radio environment requires frequent re-clustering and maintenance overhead. The gain by clustering can be mitigated by energy-consumption due to re-clustering and maintenance overheads. In this chapter, we present an event-driven spectrum-aware clustering protocol for CRSN. Overheads can be decreased by exploiting event-driven nature

of CRSN. This decrease is achieved by forming clusters in the corridor between event region and sink after detection of an event. We also aim to form connected clusters in order to avoid isolated entities. We perform mathematical study to find average re-clustering probability of a cluster in our network setup.

The remainder of this chapter is organized as follows. Section 2.2 presents the related work, and Section 2.3 explains network model. In Section 2.4, we describe our protocol by explaining determination of eligible nodes, clustering algorithm and control overheads of the protocol. In Section 2.5, impact on re-clustering is explained by event-driven nature of our approach. We present performance evaluation in Section 2.6.

2.2 Related Work

In this section, we describe related work in the literature on clustering for CRN and WSN. The authors in [22] propose a distributed coordination architecture to overcome spectrum heterogeneity challenge and scalability issues. The proposed scheme groups nodes according to the selection of coordination channels adaptively. It tries to maintain the groups during the network operation. Users are clustered in the same group if they have at least one common channel and two nodes in the same cluster can communicate via multiple hops. The aim is to minimize the number of clusters in the network. However, it decreases the number of common channels in clusters. Consequently, this feature of this protocol increases re-clustering probability since it causes less common channels among the cluster members. In [23], the network is partitioned into clusters by grouping neighbor nodes sharing local common channels. The network is formed by interconnecting the clusters gradually. Furthermore, it proposes a hybrid MAC protocol where the channel access time is divided into superframes which have intervals for inter-cluster and intra-cluster communication. Furthermore, it provides mechanisms for neighbor discovery, cluster formation, network formation, and network topology management. [26] uses graph theory for spectrum opportunistic clustering (SOC) and assigns control channel to each cluster so that each node in a cluster can communicate within the cluster by local common channels. The recent work [27] presents network topology and spectrum availability as bipartite graphs. Every node constructs bipartite graphs with its one-hop neighbors and available channels. Biclique graphs are obtained from these bipartite ones accord-

ing to metrics such as maximum edge, maximum node and maximum edge one sided cardinality. These approaches do not use common channel over the entire network, however, control channel is assigned to each cluster in the network by the clustering technique. Through the assigned control channel intra-cluster communication is performed. The authors in [28] construct minimal number of clusters in cognitive radio networks using affinity propagation (AP) message-passing technique. ROSS-DGA and ROSS-DFA are distributed clustering approaches offered in [5]. They form robust clusters by providing inter- and intra-cluster connectivity using game theory.

The recent work in [30] suggests a spectrum-aware clustering protocol to enable energy-efficient communication in CRSN by intra-cluster aggregation and inter-cluster relaying. It also finds the optimal number of nodes in a cluster.

Despite vast amount of clustering approaches in WSN, the idea of clustering between event and sink is first proposed in [31], namely Event-to-Sink Directed Clustering (ESDC). It suggests forming clusters in corridor between the event and the sink in WSN. However, this clustering scheme is not applicable to CRSN since WSN nodes are not aware of CR functionalities and it does not address spectrum heterogeneity.

Although there exists significant amount of clustering approaches on cognitive radio networks, they do not address the challenge of limited energy resource and hardware capacity of sensor nodes. Thus, energy-efficient clustering solution is required to address the limited energy resource challenge as well as opportunistic spectrum access challenges.

2.3 Network Model

2.3.1 Cognitive Radio Model

Sensors with cognitive radio capability and primary users coexist in CRSN. Cognitive radios (CRs) are secondary users (SU) which can opportunistically access licensed channels if there is no primary user activity [2].

There are C non-overlapping orthogonal channels having unique ID. CR nodes can detect vacant spectrum bands by spectrum sensing. Spectrum readings provide perfect results and vacant spectrum bands do not change during clustering process. The clustering is performed according to

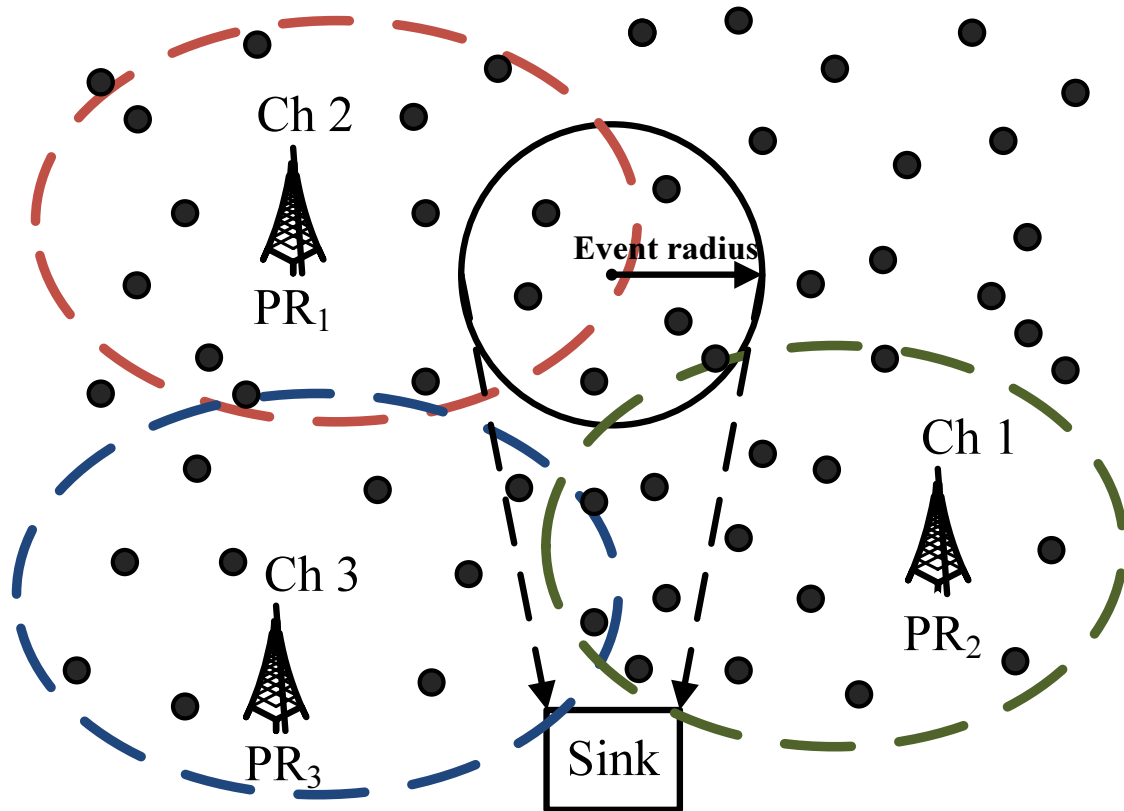


Figure 2.1: Typical CRSN topology with event and sink.

the snapshot of the network and vacant spectrum bands. Sensing results of SUs are correlated for the same neighborhood, however it may change due to the temporal activities of PUs.

Traffic in CRSN is event-driven. Sensor nodes within event radius detect event. Many-to-one traffic pattern toward one sink node is generated as illustrated in Fig 2.1. There are 3 primary users (PUs) and the coverage of them are designated by dashed circles and their operating channel is shown in Fig 2.1. Inside these circles, secondary users (SUs) can not use those channels. Event detecting nodes are the nodes within the event radius. These nodes generate packets to delivered to the sink. Arrows indicate the data flow from the event to the sink.

Clustering needs the exchange of control messages. This message exchange is provided via common control channel. It is available for SUs at any time [32]. SU can access the channels

by a CSMA/CA-based medium access protocol. Overlay spectrum sharing is used as interference avoidance model, i.e., SUs use portions of the spectrum not used by the PU [2]. Furthermore, SU nodes know their location by utilizing localization algorithms.

Neighbor discovery is provided by the common control channel signaling periodically. By this signaling, all nodes know one-hop and two-hop neighbors and their vacant channels. In this chapter, we are interested in CRSN in which nodes are stationary, therefore, one-hop and two-hop neighbors do not change unless they deplete resources. Hence, only their available spectrum bands change. Let N_i^1 denote one-hop neighbor list of node i and N_i^2 two-hop neighbor of it. C_i represents the vacant channels of the node i . Table 2.1 shows the notations and their explanations which are useful for explaining the clustering protocol.

2.3.2 Primary Channel Usage Model

As in [33, 34, 35], the traffic of primary channel c is modeled as semi-Markov ON-OFF process where channel c 's state changes with arrival rate λ_c and departure rate μ_c as shown in Fig. 2.2. OFF state of channel c is considered spectrum opportunity for secondary users in the system. Secondary users can exploit by utilizing this channel for communication or cluster formation. ON and OFF periods for channel c follows exponential distribution and they are independent.

The steady state busy probability of the channel c is given by

$$p_{busy}^c = \frac{\lambda_c}{\lambda_c + \mu_c}. \quad (2.1)$$

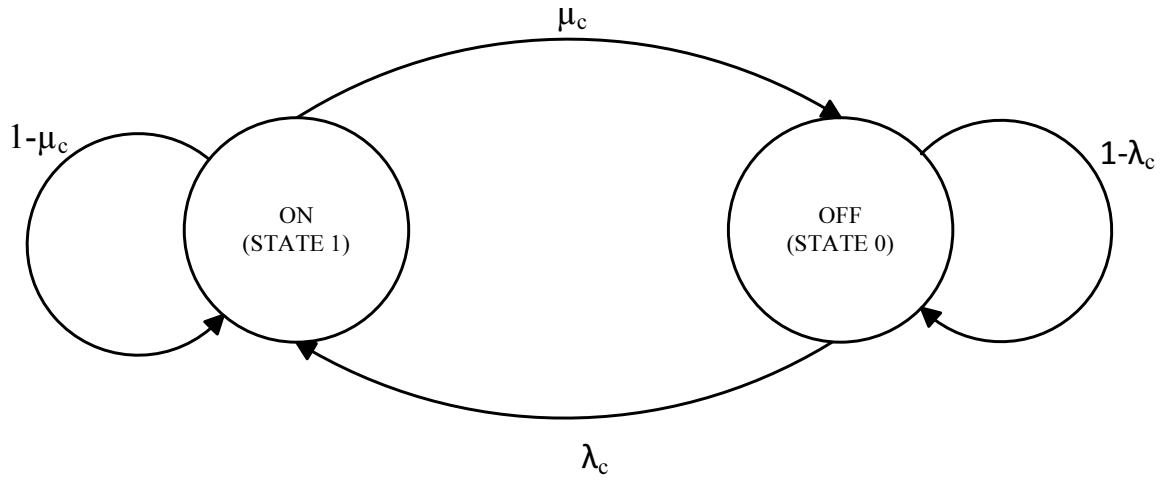
In multi-channel radio environment, clusters are formed according to vacant spectrum band. They are valid until at least one common channel is present among cluster members. Re-clustering is required if the cluster-head loses its communication with its members through common cluster channels. The channel usage pattern is assumed to follow i.i.d. ON/OFF random process. According to this, the probability that no channel is idle in the system

$$Pr[No\ idle\ channel] = \prod_{i \in C} p_{busy}^i. \quad (2.2)$$

Table 2.1: Notations For Clustering Protocol

Notation	Explanation
N	Number of secondary nodes in the network
S	Set of secondary nodes in the network
C	Set of channels in the network
N_i^k	k hop neighbor list of node i
C_i	Available channel list of node i
$d_{i,j}$	Euclidean distance between nodes i and j
d_i^e	Eligible node degree of node i
P_i	Weight for cluster-head selection , $ C_i \times d_i + 10 / d_{i,sink}$
$CN_i[k]$	Cluster nodes whose cluster-head is node i at cluster formation iteration k
$CC_i[k]$	Common channels for the cluster constructed by the cluster-head i at cluster formation iteration k
$CD_i[k]$	Max. eligible two-hop neighbors accessible through a channel $\in CC_i[k]$ and $CN_i[k]$ at cluster formation iteration k
$N(i)$	Cluster member nodes whose cluster-head i
$C(i)$	Cluster channels whose cluster-head i
R	Event radius in meters
D_{es}	Distance between event and sink in meters
r	Cognitive radio transmission range in meters
T_{cls}	Time in msec to form cluster by eligible nodes after detection of an event

Cognitive radios in the cluster have the capability to fully observe the N channels. Therefore, no states are hidden to the cluster-head which is responsible for spectrum coordination.

Figure 2.2: Semi-Markov model for channel c .

2.4 Event-driven Spectrum-Aware Clustering (ESAC)

In this section, we explain our coordination scheme which is in fact event-driven spectrum-aware clustering protocol for CRSN. In cognitive radio sensor networks, packets are generated by the event-detecting nodes. Afterwards, the packets are routed to the sink. Hence, coordination scheme is needed between event and sink. The coordination is provided by our clustering protocol for CRSN. In order to establish this coordination between event and sink, we propose two phase protocol. The first phase is for the determination of the intermediate eligible nodes between event and sink, i.e., eligibility corridor. In the second phase, the nodes in this corridor form the spectrum-aware cluster with their one-hop neighbors. Clusters are maintained until the end of the event. These phases are explained individually in the following subsections.

2.4.1 Determination of Eligible Nodes For Clustering

Traffic in CRSN occurs when an event exists. Therefore, resources are used in the network for event occurrences. The communication need triggers our protocol. In the first step of our protocol is to determine the corridor between event and sink. We specify this corridor in distributed manner in the decentralized cognitive radio sensor network. We establish this corridor by changing the status

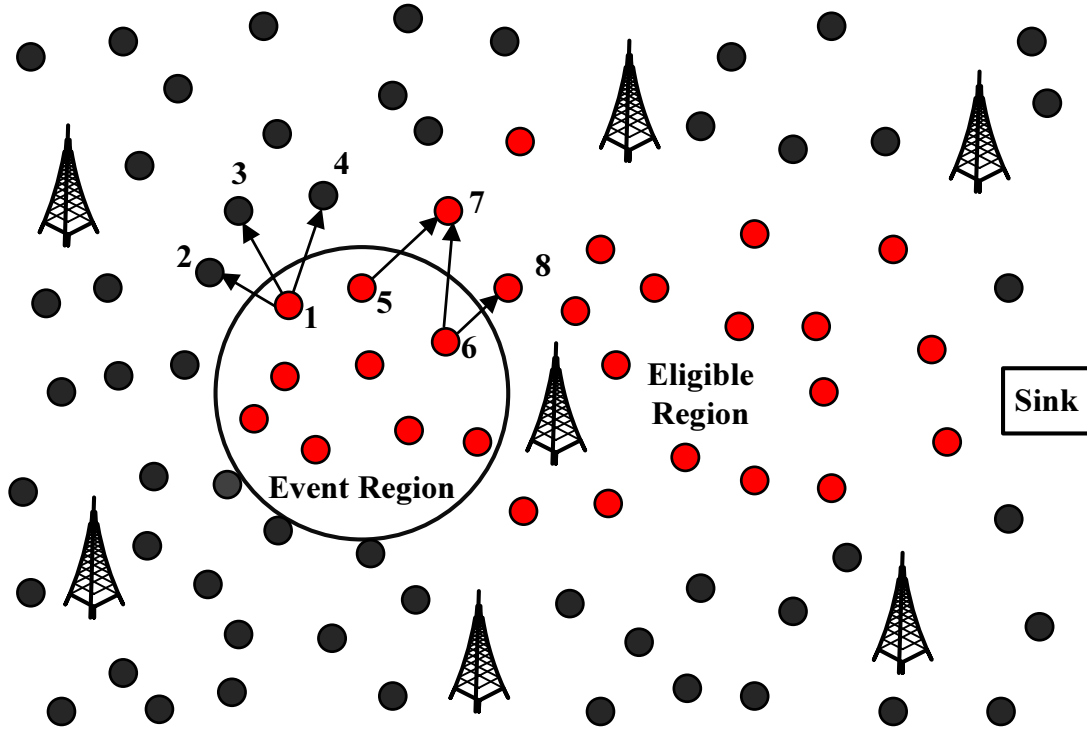


Figure 2.3: Illustration of an eligibility scenario.

of the nodes in this region. In this distributed approach, the first step of determining the eligible nodes is the event detection. The event detecting nodes become eligible for clustering directly. Afterwards, Eligibility For Clustering REQuest (EFC_REQ) messages are sent by these nodes to their one-hop neighbor through common control channel. Nodes receiving this message determine to be an eligible node according to the condition to be located closer to the sink and farther to the event location than the EFC_REQ sender. The new eligible nodes send EFC_REQ to their non-eligible one-hop neighbors and the process continues until EFC_REQ reaches the sink. Non-eligible nodes do not send EFC_REQ message, hence, the corridor can not be expanded further by these nodes. Algorithm 1 outlines the eligibility process for clustering. ESAC determines eligible nodes in a distributed manner by Algorithm 1.

Algorithm 1 Determination of the Eligible Nodes for Clustering

```

1: Consider node  $i \in S$  where  $S$  is set of nodes in the network
2: if Node  $i$  detects event then
3:   It is eligible for clustering
4:   State( $i$ ) = "Eligible Ordinary Node"
5:   Start sending EFC_REQ to one-hop neighbors other than event detecting neighbors
6: else
7:   if It receives EFC_REQ from its neighbor then
8:     Compare the distance
9:     if  $d_{i,sink} \leq d_{EFC\_REQ-sender,sink} \wedge d_{i,event} \geq d_{EFC\_REQ-sender,event}$  then
10:      Node  $i$  is eligible for clustering
11:      State( $i$ ) = "Eligible Ordinary Node"
12:      Send EFC_REQ to one-hop neighbors
13:    else
14:      Not eligible
15:    end if
16:  else
17:    Node  $i$  is not eligible
18:  end if
19: end if

```

An eligibility scenario is illustrated in Fig. 2.3. A number of CRSN nodes randomly deployed in this network and event region is shown by a circle. Eligibility region is determined according to Algorithm 1. In this scheme, the event detecting nodes become eligible instantly. These nodes are located inside the event circle. The nodes in the event detecting region start sending EFC_REQ immediately to their non-eligible one-hop neighbors. This request is disseminated through eligible nodes to the sink.

Only eligible nodes send EFC_REQ to their one-hop neighbors. After the detection of the event, the nodes in the event region sent first EFC_REQ messages to its neighbors as shown in Fig. 2.3. Node 1 sends EFC_REQ to its neighbors 2, 3, and 4. However, nodes 2, 3, and 4 cannot join the clustering since they are not closer to the sink than the node 1. Node 6 sends EFC_REQ to nodes 7 and 8. The node 7 cannot join clustering by the request from node 6 since node 7 is farther to the sink. However, node 7 joins the clustering due to the EFC_REQ from the node 5. The state of the eligible nodes is determined to be “Eligible Ordinary Node”. These request messages flow through eligible nodes until they reach to the sink. In the end of this process, red-colored nodes are the corridor nodes joining communication. Other nodes are not eligible, and hence they do not consume energy for clustering.

A node knows its neighbors, their locations and available channels. This information is periodically updated by neighbor discovery process. If a node receives an EFC_REQ message by one of its neighbors, the sender already knows if the request receiver is eligible. However, the nodes that are eligible or non-eligible for clustering inform their neighborhood by Eligibility For Clustering REPLY (EFC_REP) message upon receiving an EFC_REQ message.

2.4.2 Clustering Algorithm

Our approach brings a new perspective for clustering by forming clusters incident to events in CRSN. The motivation of clustering in sensor network is to create organizational structures and to manage distributed network in a structured way. In this chapter, we group the nodes according to their spectrum availabilities while maintaining communication between intra-cluster and inter-cluster nodes. Only the nodes that are appointed as eligible form clusters. In our approach, clusters are not maintained in the network if event detecting nodes do not further sample the event.

If an eligible node knows the eligibility condition of its neighbors, it initiates clustering process which is explained in Algorithm 2. The clustering algorithm is inspired by [26]. Our clustering protocol is cluster-head first protocol, and there is an additional constraint that cluster-heads maximize the number of two-hop members that they can reach by its one-hop members through the cluster channels. We decrease control overhead for constructing the clusters by means of cluster-head first algorithm since there are not extra control message exchanges for selecting cluster-heads. Furthermore, we form non-isolated clusters by considering two-hop eligible members. This feature provide clusters to communicate with each other by their one-hop neighbors. Eligibility for clustering and spectrum-aware clustering processes work sequentially such that eligible nodes immediately start forming clusters after having full knowledge about the eligibility of its one-hop members.

In dynamic radio environment, the clusters are formed according to the spectrum band availabilities. The nodes which have similar vacant spectrum band are grouped in the same cluster in the same spatial neighborhood. In our clustering scheme, every eligible node is assigned to a weight which is calculated as $P_i = |C_i| \times d_i^e + 10 / d_{i,sink}$. In this weighting structure, we regard the node degree, available channel, and the distance to the sink. The node i with the highest weight P_i in its one-hop neighborhood is chosen as cluster-head. A node which has the highest weight in any of its one-hop neighbor list can also become a cluster-head. By this weighting method, we select the nodes which have higher eligible node degree and available channel, and which are closer to the sink in its neighborhood.

Cluster-heads form clusters by selecting appropriate vacant channels and one-hop neighbors. Our protocol maximizes the number of two-hop neighbors that can be reached by cluster-heads through cluster members over cluster channels. If a node i becomes a cluster-head, it tries to maximize the product of three terms for the constructed cluster, which is $|CN_i| \times |CC_i| \times |CD_i|$.

In the clustering procedure, cluster-head node i firstly determines the weight of every channel C_i . The weight of a channel of node i is the number of one-hop neighbors that node i can reach through that channel. Node i firstly adds the channel which has the highest weight to $CC_i[1]$. The index number shows the iteration of the algorithm. Hence, in the first iteration the index number is [1]. If two or more channels have the same weight, we break tie by choosing the channel having the least channel ID.

Algorithm 2 Spectrum-Aware Clustering Algorithm in CRSN

```

1: if State(i)=="Cluster-head" then
2:    $k = 0$  and  $CC_i[k] = \emptyset$  and  $CN_i[k] = N_i^1$ ;
3:   for  $j \in C_i$  do
4:     Find the channel  $j$  having highest overlap with  $N_i^1$  in  $C_i - CC_i[k]$ 
5:      $k \leftarrow k + 1$ 
6:      $CC_i[k] = CC_i[k - 1] \cup \{j\}$ 
7:     if  $|CC_i[k - 1]| = 0 \wedge CN_i[k - 1] = \emptyset$  then
8:       break;
9:     else
10:      Find the nodes that have the vacant bands of  $CC_i[k]$ ;
11:       $CN_i[k] = \{ \text{One-hop neighbor CRs having } CC_i[k] \text{ in their vacant bands } \}$ 
12:      Find the two-hop neighbors  $CD_i[k]$  such that  $i$  reaches through the  $CC_i[k]$  and  $CN_i[k]$ 
13:       $CD_i[k] = \{ \text{One-hop neighbor other than } CN_i[k] \text{ having } CC_i[k] \text{ in their vacant bands } \}$ 
14:    end if
15:     $w_i[k] = |CN_i[k]| \times |CC_i[k]| \times |CD_i[k]|$ 
16:  end for
17:  Find maximum weight  $w_i[k]$  ;
18:  if there are more than one iteration having the maximum weight then
19:    Select the one with highest number of cluster member  $CN_i$ 
20:  end if
21:  Return  $N(i) = CN_i[k]$  and  $C(i) = CC_i[k]$ ;
22:  Send C_REQ to the nodes in  $CN_i[k]$ 
23:  Wait for C_REP messages from  $CN_i[k]$  to finalize cluster membership
24: else
25:   if State(i)=="Eligible Ordinary Node" then
26:     Wait for C_REQ
27:     Join the cluster which has the maximum weight among C_REQs
28:   end if
29: end if

```

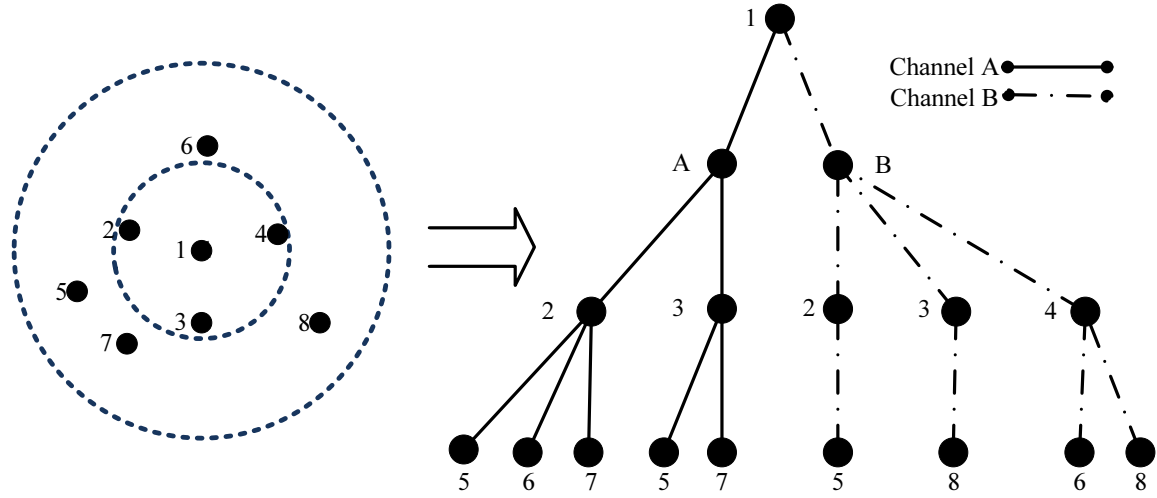


Figure 2.4: One-hop and two-hop neighbors of cluster-head node 1 and its constructed tree.

The channel that has the highest weight is added to $CC_i[1]$ and the nodes having this channel in their available channel list are added to $CN_i[1]$. We find the number of two-hop neighbors that the node i can reach via nodes in $CN_i[1]$ over channel $CC_i[1]$. These two-hop neighbor nodes are added to $CD_i[1]$. The weight of first iteration is $w_i[1]$ which is the product of $|CN_i[1]|$, $|CC_i[1]|$ and $|CD_i[1]|$. In the second iteration, $CC_i[2]$ becomes $CC_i[1] \cup \{j\}$ where j is the second highest weighted channel. $CN_i[2]$ contains the one-hop neighbor nodes having vacant channels which are the elements of $CC_i[2]$. $CD_i[2]$ is found by determining accessible two-hop neighbors by the nodes in $CN_i[2]$ over channels in $CC_i[2]$. The weight of this iteration is found as in the previous weight calculation. This process continues until k^{th} step which results in $CN_i[k-1] = \emptyset$ or $|CC_i[k-1]| = \emptyset$. In the end, cluster-head i chooses the iteration having the highest weight. Finally, $N(i)$ is set of cluster nodes constructed by node i and $C(i)$ is the channels common for the nodes in $N(i)$. The steps can be seen in Algorithm 2.

Fig. 2.4 shows a tree constructed by cluster-head node 1 in order to determine cluster members and cluster channels. In the first level, two branches denote the vacant spectrum bands of cluster-head node 1. Available channels of cluster-head node 1 are A and B . The second level shows the one-hop eligible nodes having channels A and B . Node 1 has the neighbor nodes 2 and 3 which

Table 2.2: Iterations for Cluster-head node 1 in Fig. 2.4

Iteration	$CC_1[k]$	$CN_1[k]$	$CD_1[k]$	$w_1[k]$
$k = 1$	$\{B\}$	$\{2, 3, 4\}$	$\{5, 6, 8\}$	9
$k = 2$	$\{B, A\}$	$\{2, 3\}$	$\{5, 6, 7, 8\}$	16

have channel A . The one-hop neighbor nodes 2, 3 and 4 have channel B . The third level shows the eligible two-hop neighbor nodes. For example, the one-hop neighbor 2 has one-hop neighbor nodes of 5, 6 and 7 having available channel of A . Since node 1 has two available channels, there are at most two iterations shown in Table 2.2. The first iteration is on the channel B since the number of one-hop neighbors having channel B is greater than that of channel A . Afterwards, channel A is added to cluster channel. According to Algorithm 2, iterations for clusters are calculated and tabulated in Table 2.2. The cluster member nodes and cluster channels of cluster-head node 1 are $N(1) = \{2, 3\}$ and $C(1) = \{B, A\}$ since the second iteration has the highest weight.

Firstly, the node 1 is selected as cluster-head since it has highest weight in its one-hop neighborhood. According to Algorithm 2, it determines the cluster structure and sends Cluster REQUEST message (C_REQ) to the nodes in $N(1)$. The nodes receiving this request acknowledge cluster-head that they are now members of cluster constructed by node 1 if cluster weight of node 1 is greater than the other received cluster weight. The nodes that are not member of any cluster can become a cluster-head itself. If a node receives more than one C_REQs, it accepts the request that has the highest weight. Cluster formation by cluster-head is completed if it knows the condition of eligible one-hop members via Cluster REPLY (C_REP) messages.

In this algorithm, we maximize the product of number of nodes and channels in the cluster, and the number of two-hop neighbors that cluster-head can directly communicate by cluster members through cluster channels. By this way, we compromise between common channels, cluster size and inter-cluster connectivity.

2.4.3 Control overheads of ESAC

In literature, the clustering schemes in cognitive radio maintain the organizational structures in the entire network disregarding event occurrences. Hence, nodes are organized for data transmission at the cost of energy. In our scheme, clusters are formed from scratch upon detection of an event. This requires exchange of control information in order to generate clusters in the corridor between event and sink. These overheads are itemized as follows:

- EFC_REQ is sent by eligible nodes to further determine the eligible nodes closer to the sink starting from event detecting nodes.
- Nodes send EFC_REP to inform one-hop neighbors whether if they are eligible for clustering.
- Cluster-head nodes send C_REQ messages to the cluster members according to Algorithm 2.
- Members validate their membership by sending C_REP message to their cluster-heads.

In order to form clusters, an eligible node except event detecting one sends EFC_REQ, EFC_REP and C_REP or C_REQ according to the node's weight in its neighborhood. Event detecting nodes do not send EFC_REP message since they are directly eligible.

2.5 On the Re-clustering Probability of a Cluster

In our approach, we form clusters according to spectrum availabilities of a cluster-head and its one-hop neighbors considering the two hop neighbors' channels for connectivity between clusters. Due to the dynamic change caused by PU activities in the spectrum availabilities, re-clustering is necessary if no common channel remains among cluster members.

Re-clustering condition for any cluster is to have no common available PU channels among the cluster members. In the below analysis, we calculate the average re-clustering probability of a cluster.

Cluster-head forms clusters with some of its one-hop members. Hence, cluster coverage region is the region covered by the cluster-head plus the extra coverage regions coming from the possible one-hop neighbors. Applying the procedure in [36], the coverage area of the cluster can be found.

The cluster-head coverage area is πr^2 as an ordinary node, and the maximum total area of cluster is $\pi(2r)^2$ since all the one hop neighbors can be located at a distance r to the cluster-head and the total radius becomes $2r$.

In this work, the sensor network is stationary. As in [36], locations of the sensor nodes are distributed according to two dimensional Poisson point process. Density of this process is determined to be as

$$\zeta = \frac{N}{A} \quad (2.3)$$

where A is the total area of the sensor network.

Let $E[CA_1]$ denote the expected coverage area of any randomly chosen cluster-head in the network where CA_1 denotes the coverage area of chosen cluster-head as first node in this process. As the cluster-head gathers more members, the expected coverage area increases. For example, after the $(k-1)^{\text{th}}$ node is accepted as a member, the total covered area becomes $CA_k = CA_{k-1} + EA_k$ where CA_k is the covered area by the cluster-head and its $k-1$ member and EA_k is the extra coverage area contributed by the k^{th} node in the cluster. The expected covered area is obtained by taking expectation of both sides

$$E[CA_k] = E[CA_{k-1}] + E[EA_k]. \quad (2.4)$$

Let FR_k is the fraction of the contribution of the k^{th} node in the cluster and is given as

$$FR_k = \frac{TA - E[CA_{k-1}]}{TA} \quad (2.5)$$

where TA is the total maximum area that a cluster can cover, $4\pi r^2$. The contribution area of the node k is $EA_k = FR_k \times CA_1$.

The equation (2.4) becomes as follows

$$E[CA_k] = E[CA_{k-1}] + E\left[1 - \frac{E[CA_{k-1}]}{TA}\right]E[CA_1]. \quad (2.6)$$

If we continue this procedure from cluster-head to the n^{th} node, the expected coverage area becomes

$$E[CA_k|k=n] = \left[1 - \left(1 - \frac{E[CA_1]}{TA}\right)^n\right]E[CA_1]. \quad (2.7)$$

k is the number of possible cluster members which has to be located within the transmission range of the cluster-head. Since the distribution of nodes are Poisson, the probability that there are n nodes

in πr^2 is

$$Pr(k = n) = \frac{e^{-\zeta\pi r^2} (\zeta\pi r^2)^n}{n!}. \quad (2.8)$$

The expected cluster coverage area $E[CCA]$ can be given as

$$E[CCA] = \sum_{n=0}^N E[CA_n | k = n] Pr(k = n). \quad (2.9)$$

Let Ω be $E[CCA]$ and Z^i is defined as the area in Ω which is covered by PU using channel i . Z^i can be given as

$$Z^i = \int_{\Omega} \xi(x) dx \quad (2.10)$$

where

$$\xi(x) = \begin{cases} 1 & \text{if point } x \text{ is covered by PU using channel } i \\ 0 & \text{otherwise} \end{cases} \quad (2.11)$$

The expected Z^i is given by

$$E[Z^i] = \int_{\Omega} E[\xi(x)] dx. \quad (2.12)$$

$$\begin{aligned} E[\xi(x)] &= Pr(\text{PU using channel } i \text{ cover point } x) \\ &= 1 - Pr(\text{No PU using channel } i \text{ cover point } x) \\ &= 1 - e^{-\psi_i \pi \Gamma^2} \end{aligned} \quad (2.13)$$

where Γ is the transmission range of a PU and ψ_i is the mean of the Poisson point process of primary users utilizing channel i .

Finally, the expected area covered by PUs using channel i on Ω becomes as

$$E[Z_i] = \int_{\Omega} E[\xi(x)] dx = (1 - e^{-\psi_i \pi \Gamma^2}) \Omega. \quad (2.14)$$

The average probability that channel i is used in the cluster area Ω is

$$\gamma_{\Omega}^i = \frac{E[Z_i]}{A} = \frac{(1 - e^{-\psi_i \pi \Gamma^2}) \Omega}{A}. \quad (2.15)$$

For re-clustering of the cluster, all channels must be occupied in the region Ω . Hence, the overall average probability that all channels are occupied in the cluster area is given as

$$\gamma_{\Omega} = \prod_{i=1}^C \frac{[(1 - e^{-\psi_i \pi \Gamma^2}) \Omega]}{A}. \quad (2.16)$$

Since all channels are independent, the overall probability is found by multiplying probabilities that the area Ω is under the coverage of PUs using each channel. The average probability that cluster-head region is covered by PUs is obtained spatially. The activities of these primary user also changes temporally which is independent of the spatial distribution. In Network Model section, PU channel usage is modeled as semi-Markov ON-OFF process and usage statistics of the channels are independent. Hence, overall average re-clustering probability is given as no idle channel in area of Ω

$$Pr[Re - clustering] = \gamma_{\Omega} \cdot Pr[No idle channel]. \quad (2.17)$$

In the network operation, formed clusters expose spectrum availability changes and this situation causes maintenance and re-clustering overhead. In order to reduce them, we propose an algorithm that decreases clustered network operation duration and number of clusters by event-to-sink approach. CRSN is an event-driven network such that data transmission begins with events, therefore, we exploit this nature by forming and utilizing clusters only in the event occurrences. This strategy reduces energy consumption without formation and maintenance of clusters in whole network. In our approach, clusters formations are related with events in the network. Hence, the re-clustering probability is decreased by event occurrence probability. The new re-clustering probability for our scheme is found as

$$\begin{aligned} Pr[Event - driven re - clustering] = \\ Pr[Event Occurrence] \cdot \gamma_{\Omega} \\ \cdot Pr[No idle channel]. \end{aligned} \quad (2.18)$$

2.6 Performance Evaluation

The performance of our protocol is evaluated in terms of eligible nodes ratio, and delay, total energy consumption, energy efficiency and connectivity. We perform simulations by using MATLAB.

2.6.1 Ratio of eligible nodes in the network

The most important advantage of our protocol is that clustering does not take place in the entire network yet occurs in the event region in addition to the corridor between event and sink. By

changing the network parameters, the fraction of the eligible nodes in the network is examined. Throughout the simulations, sink is placed at $X = 0$ m and $Y = 50$ m in 100 m x 100 m network field. In the simulations, the results are averaged over 50 different topologies. In the first simulation setup, by increasing the distance between event and sink, we investigate the ratio of the eligible nodes with different event radius. Event is generated on the $Y = 50$ m line, 200 CR nodes are distributed uniformly and transmission range of nodes is set to 20 m. Fig. 2.5 shows that only under 30% of the nodes in the network join the clustering when the event to sink distance is 20 m for an event radius 30 m. If event radius is 10, the fraction is below 10%. The fraction goes over 90% if event radius is 30 and the distance between event and sink is above 60. For this case, due to large event radius substantial number of nodes whose distances to sink are above 60 become eligible, and those nodes and their neighbors increase the fraction of eligible nodes. On the other hand, for events with radius of 10, even if distance between the event and the sink is 60, fraction of eligible nodes is 55%. As seen in Fig. 2.5, a considerable number of nodes do not join clustering for small event to sink distances, hence these nodes do not consume energy due to clustering.

In the second simulation setup, in a 100 m x 100 m network field, different number of CRs are deployed uniformly while event radius is 30 m and transmission range of CR is 20 m. For this setup,

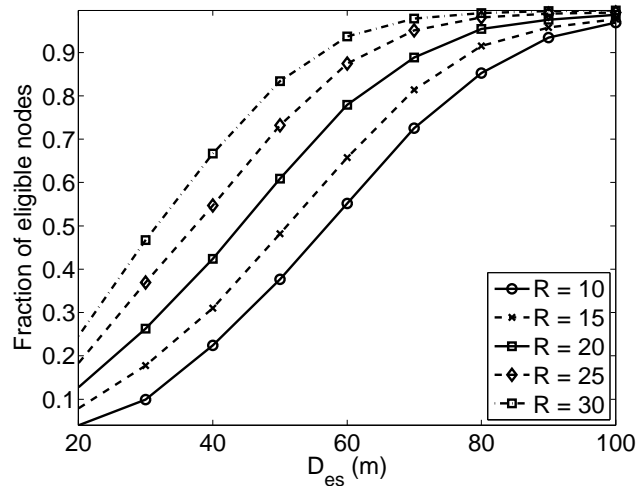


Figure 2.5: Fraction of eligible nodes in the network vs. D_{es} for different R (m) when $r = 20$ m and $N = 200$.

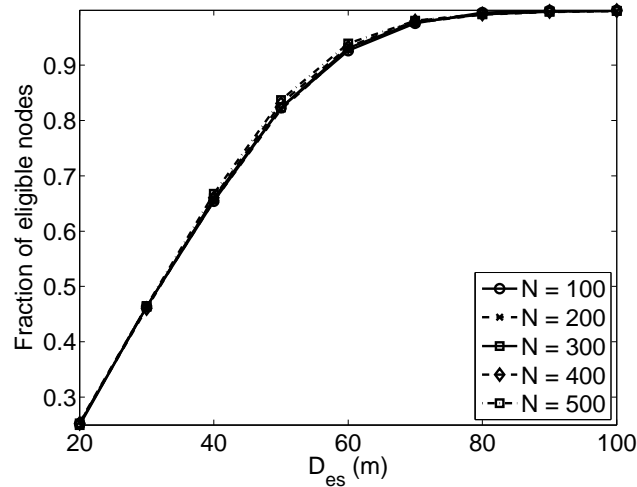


Figure 2.6: Fraction of eligible nodes in the network vs. D_{es} for different N when $r = 20$ m and $R = 30$ m.

the fraction of eligible nodes does not change significantly since CR transmission range which is 20 m does not change the region between event and sink for different number of nodes. Fig. 2.6 shows this effect such that fractions of eligible nodes are almost the same for different number of nodes and for CR transmission range 20 m. As the distance between event and sink increases, fraction of eligible node increases.

In the third simulation setup, the variation in transmission range of nodes is investigated with respect to the ratio of the eligible nodes. 200 CR nodes are distributed uniformly and event radius is fixed to be 20 m. As shown in Fig. 2.7, the rise in the transmission range of CR increases the number of eligible nodes. An eligible node makes more of its neighbor nodes eligible since its node degree increases due to the rise in transmission range. More eligible nodes mean higher of fraction of eligible nodes in the network.

In the simulations, we observe that the increase in CR transmission range and event radius causes raise in the fraction of eligible nodes in the network. On the other hand, the increase in network density does not change the fraction since transmission range of CR is enough to determine the same region between event and sink. Since the nodes are uniformly distributed and the area of the eligible nodes does not change, the fractions for different network densities are the same.

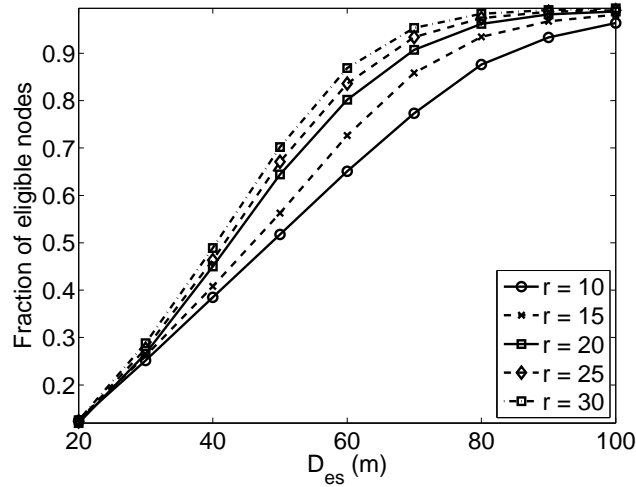


Figure 2.7: Fraction of eligible nodes in the network vs. D_{es} for different r (m) when $R = 20$ m and $N = 200$

2.6.2 Delay, Energy and Connectivity

In this section, we investigate our protocol performance in terms of delay to form clusters, energy consumed due to control signaling between eligible nodes and the connectivity between cluster-head and its two-hop neighbors. For this simulation setup, control channel's bandwidth is assumed to be 512 kbps [37] and the length of the control packet is 200 bits. The environment is collision free in order to realize the effect of control signaling only. There are 10 orthogonal non-overlapping channels. 200 nodes and 20 primary users are distributed uniformly over an area 100 m x 100 m. Transmission range of a PU is 30 m.

The cumulative delay for different scenarios due to cluster formation is investigated. In this process, the causes of the cumulative delay, i.e., clustering time (T_{cls}), are determining eligible nodes and forming clusters. If an eligible node i knows the eligibility condition of its one-hop neighbors by EFC_REP messages, it determines whether it is a cluster-head according to its weight P_i . If it is cluster-head, it computes its clustering set according to Algorithm 2. It asks the nodes in clustering set to join its cluster. The nodes accepting to be a member of that cluster notify the cluster-head and its neighborhood.

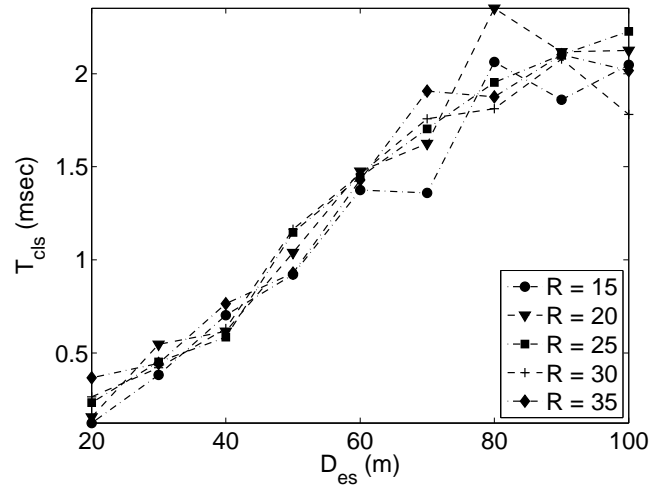


Figure 2.8: T_{cls} (msec) vs. D_{es} (m) for different R (m) when $r = 20$ m and $N = 200$.

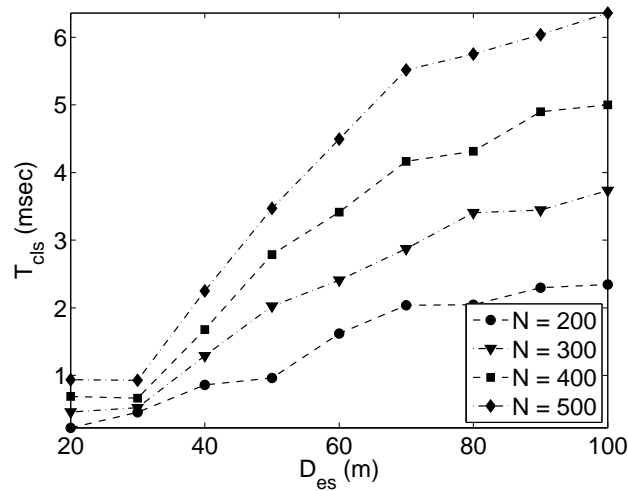


Figure 2.9: T_{cls} (msec) vs. D_{es} (m) for different N when $R = 30$ m and $r = 20$ m.

As the event radius increases, time required to form clusters do not differ considerably for different event to sink distance as shown in Fig. 2.8. Event radius is not important for the delay since the nodes in the event region are immediately start to form cluster due to becoming eligible after the detection of the event. In this case, as the distance between event and sink increases, the time

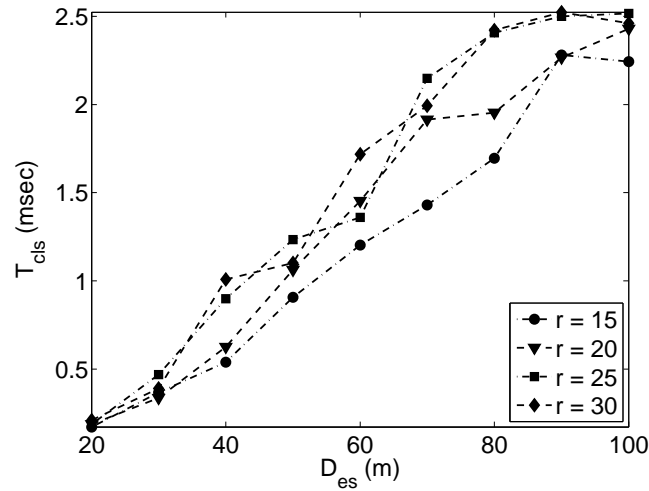


Figure 2.10: T_{cls} (msec) vs. D_{es} (m) for different r (m) when $R = 20$ m and $N = 200$.

required to form clusters rises since number of hops between event and sink increases.

In Fig. 2.9, the rise in node density increases the number of eligible nodes, and this raises the clustering time since more nodes are required to exchange control signals to form clusters. Unlike fraction of eligible nodes, clustering time rises for increasing node density.

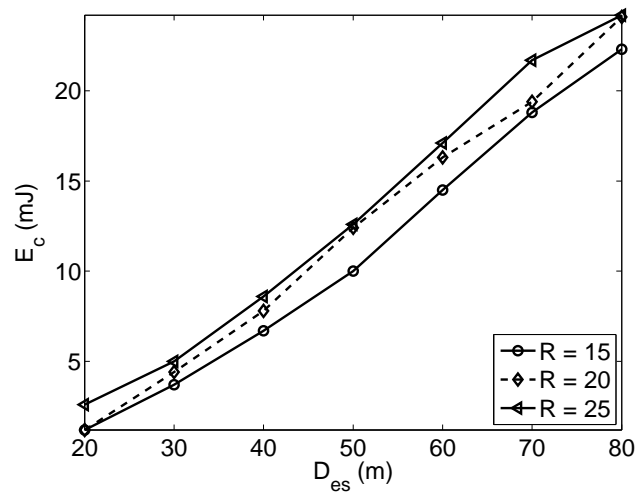


Figure 2.11: E_c (mJ) vs. D_{es} (m) for different R (m) when $r = 20$ m and $N = 100$.

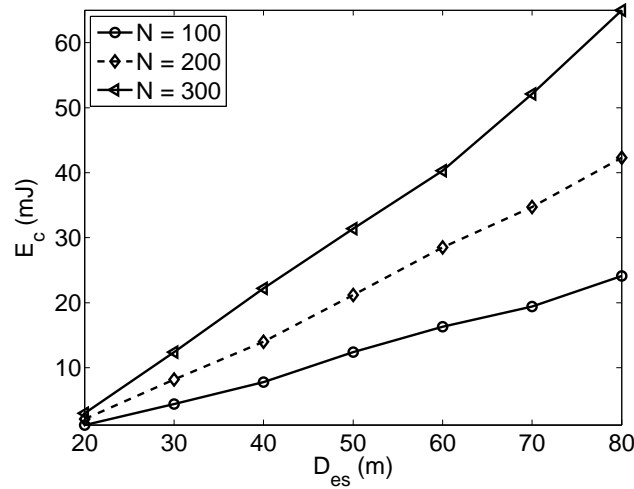


Figure 2.12: E_c (mJ) vs. D_{es} (m) for different N when $R = 20$ m and $r = 20$ m.

In Fig. 2.10, for different CR transmission range, delay changes. The increase in number of neighbors with increasing transmission range results in more nodes to be clustered. Therefore, clustering time for $r = 15$ m is smallest among the others and the clustering time for $r = 30$ m is generally higher than the others. Fig. 2.8, 2.9, and 2.10 show that clustering time increases significantly with respect to number of nodes (N) and distance between event and sink (D_{es}).

In our scheme, we try to establish a coordination among the nodes between event and sink for each event occurrences. This requires energy consumption for this coordination. In our simulations, free space path loss model is adopted such that $\epsilon_{fs} = 10pJ/bit/m^2$ and $E_{elec} = 50nJ/bit$ [38]. We investigate total energy consumption for coordination by changing event to sink distance and other network parameters. In energy consumption scenario, 200 nodes are deployed randomly in network field.

Fig. 2.11 shows slight increase in E_c . It is the natural result of the Fig. 2.8 since more nodes are performing clustering operations due to increase in event radius.

As shown in Fig 2.12, control signal transmissions increase since more nodes join clustering as network density rises. If we raise the CR transmission range, more nodes become eligible and try to form cluster. Hence, there is slight increase in total consumed energy especially for D_{es} greater than 30 m as shown in Fig. 2.13.

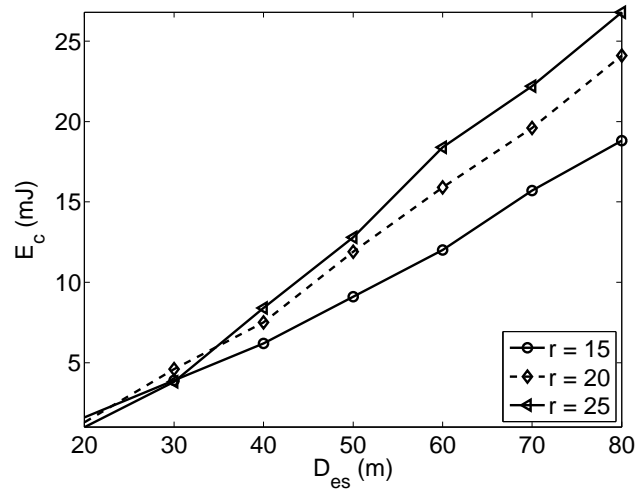


Figure 2.13: E_c (mJ) vs. D_{es} (m) for different r (m) when $R = 20$ m and $N = 200$.

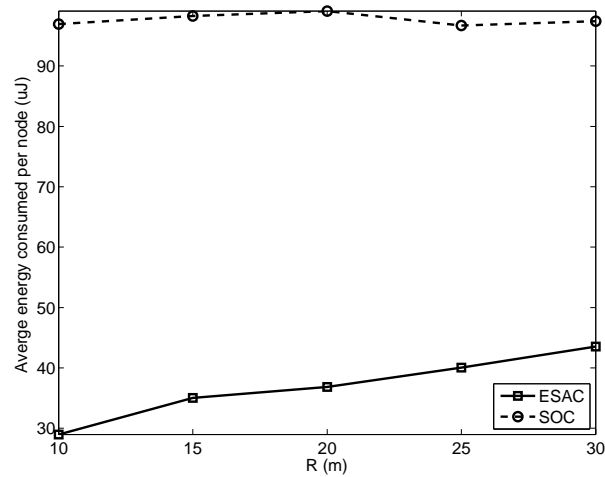


Figure 2.14: Average energy consumed per node (μ J) vs. R (m) ($N = 200$ and $r = 15$ m)

We also perform simulations to study the energy consumption of the nodes to form clusters during an event process that is generated at $X = 50$ m and $Y = 50$ m. 200 CR nodes and 20 PU nodes are distributed randomly and there are 10 licensed channels. Transmission ranges of PU and CR are 30 and 15, respectively. According to this setup, average energy consumed per event by a node in

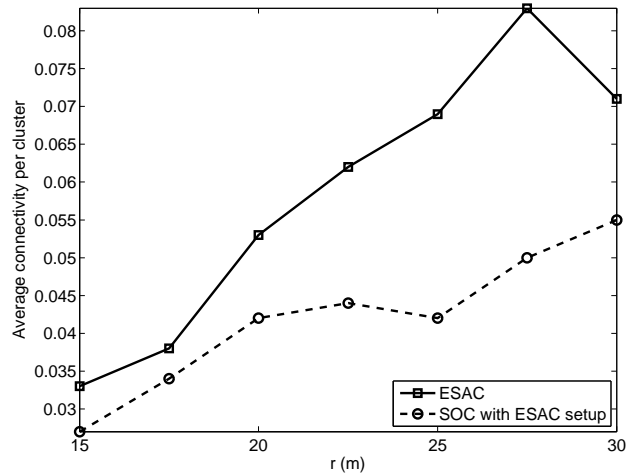


Figure 2.15: Average connectivity per cluster vs. r (m) ($N = 200$ and $R = 20$ m)

ESAC is less than SOC as shown in Fig. 2.14 since SOC forms clusters in the entire region and it is more prone to re-clustering due to dynamic radio environment. SOC re-clustering rate is taken as 0.2 in our simulations. In ESAC, clusters are formed in the corridor between event and sink and not maintained after the event. ESAC uses network resources when communication exists in the region between event and sink, hence, our protocol is more appropriate in terms of energy consumption for sensor networks which are event based systems.

Connectivity of clusters is an important metric for valid cluster formations. We define the cluster connectivity as the the number of two-hop nodes that cluster-heads can communicate with by its members through cluster channel normalized by total eligible nodes in the network. Our algorithm aims to maximize the number of two-hop neighbors which are the members of neighbor clusters having common channels with the cluster-head. In this simulation setup, event is generated at $X=100$ m and $Y=50$ m, CR transmission range is varied during simulation. Fig. 2.15 shows that our algorithm performs better than the SOC algorithm if it is applied in ESAC configuration. In other words, not considering two-hop neighbors in ESAC results in degradation in connectivity. The condition of maximizing accessible two hop members for connectivity make ESAC performance better than SOC algorithm used in ESAC configuration.

Chapter 3

ON THE EFFECTS OF NETWORK CODING IN COGNITIVE RADIO SENSOR NETWORKS

The integration of cognitive radio module with sensor nodes have revealed a new networking paradigm, i.e., cognitive radio sensor networks [4]. The challenges posed by sensor networks are amplified by the union with cognitive radio capability. Network coding is a novel technique improving capacity by combining multiple flows into one flow. In this chapter, we investigate the effects of network coding in cognitive radio sensor networks. We consider event-driven communication scenario for CRSN operation. In our simulations, CRSN benefit from the network coding technique to facilitate energy-efficient and reliable many-to-one communication.

3.1 Introduction

Demand on wireless communication has revealed the inefficient use of the electromagnetic radio spectrum due to the fixed frequency assignment approach. This situation triggered the use of dynamic spectrum access (DSA) schemes in wireless communications. DSA enabling technology is cognitive radio [2, 3, 39]. With the cognitive radio (CR) capability, wireless nodes can detect the spectrum vacancies, and utilize these radio frequencies for communication. The unique features of CR capability overcome the spectrum scarcity challenge and increase the spectrum utilization efficiency.

The adoption of cognitive radio capability in sensor networks introduces a new networking paradigm called Cognitive Radio Sensor Networks (CRSN) [4]. Sensor nodes sense the spectrum to determine the vacant channels. They have the capability to change the spectrum parameters after determining the communication channel. These operations are the vital tasks of the cognitive cycle [3]. Cognitive capability of wireless sensor nodes enable opportunistic access to the spectrum. Improvement on spectrum utilization matches the unique requirements of resource-constrained multi-hop

wireless sensor networks (WSN). Multiple channel usage availability of CRSN nodes overcomes the problem of spectrum scarcity due to the dense deployment of sensor networks. These features show the communication potentials and the challenges of CRSN. Furthermore, they point out that CRSN stands as an promising and important networking architecture.

There is an emerging body of studies on CRSN. Recent studies focus on channel management schemes in an efficient manner [6], transport layer in CRSN [7], channel assignment schemes [5], wideband spectrum sensing [40], packet size optimization [8], power and rate adaptation for maximization of information theoretical capacity [9], delay performance analysis [10]. However, to the best of our knowledge, no attempt has yet been made to investigate the effects of network coding in cognitive radio sensor networks.

Low-processing ability and energy-constraint challenges are the two key challenges of wireless sensor networks. The cognitive capability of the sensor nodes in CRSNs amplifies the challenges owned by WSN due to DSA capability. A CRSN node can not interfere with the communication of primary users. Packet loss due to spectrum mobility is an important challenge among them. Furthermore, the communication between nodes can be interrupted due to spectrum sensing and spectrum management issues raise due to DSA capability. Network coding is a novel technique to increase reliability and throughput in wireless networks. In this chapter, we apply network coding technique to observe the effects on the reliability of the event-to-sink communication and the energy consumption for this communication. Event readings of the sensor nodes are combined in the way to the sink by intermediate nodes between the event and the sink. While the generated packets in the event region are transmitted to the sink, the intermediate nodes opportunistically listen the channels in order to receive them for network coding operation. Thus information extent of the packets increases as packets are transmitted in multi-hop manner as they get close to the sink. However, as the packet extent increases by mixing more source packets, the decoding complexity increases. If information extent of the packet is low, then the network coded packets may be redundant such that some packets are linearly dependent.

In this chapter, we investigate the response of CRSN in terms of energy efficiency and reliability when using network coding. Network coding is a well investigated technique for communication networks [41, 42, 43, 44]. It has been suggested to achieve max-flow capacity for multicast commu-

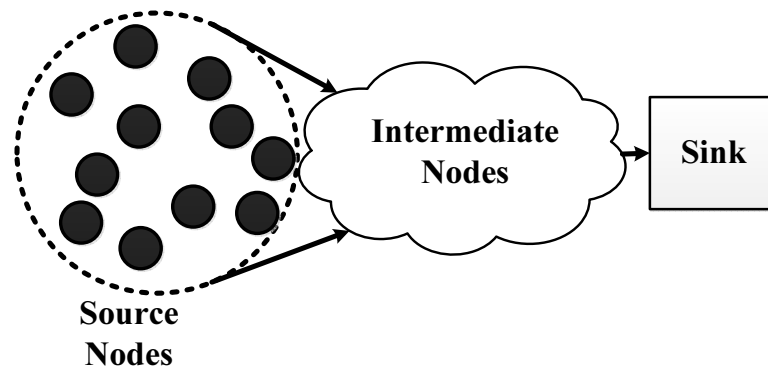


Figure 3.1: Abstraction of a sensor network scenario where multiple nodes send packets to the sink.

nication [41]. The network coding studies can be divided into theoretical [43, 44], simulation-based [53, 54], and implementation based [46] classes. None of these works studies the applicability of network coding in CRSN taking into account the challenges of cognitive radio capability and the resource-constraint of sensor network challenges. Our chapter relies on simulation-based study scrutinizing the positive and negative effects of network coding and investigating the applicability of this novel technique with respect to energy efficiency and reliability.

In our setup, CRSN adopts event-driven scenario where readings of the sensor nodes in the event region are transmitted in multi-hop manner to the sink as shown in Fig. 3.1. During the data transmissions, nodes choose best available channel among the vacant bands. Furthermore, in our scenario, the communication occurs in the region between the event and the sink. Every node in this region searches for coding opportunity. Due to the broadcasting nature of wireless CRSN nodes, some of the event nodes and the intermediate nodes can exploit the coding opportunities. However, the intermittent connection of CRSN imposes a dynamic behavior on network coding since the incoming links of an intermediate node may fail due to the changes in channel availability. This situation has effects on energy-efficiency and latency. Based on the explained scenario, we investigate how much network coding is beneficial for CRSN architecture.

The remainder of this chapter is organized as follows. In Section 3.2, the system model is represented. Background information about network coding is provided in Section 3.3. The effects of network coding is explained by simulation study in Section 3.4.

3.2 System Model

3.2.1 Network Model

A cognitive radio sensor network consists of two types of network. CRSN nodes form secondary network, and primary users (PUs) form the primary network. PUs use the licensed channels without any restriction, however, cognitive radios opportunistically access the spectrum bands with their DSA capabilities. Data gathering is triggered by the event. Information flow is from event to sink through the intermediate nodes.

We consider a CRSN network with N stationary CRSN nodes. M number of non-overlapping orthogonal licensed channels are potentially available for a CRSN node in the network. These channels have the same bandwidth. The communication environment is assumed to be collision-free. CR-enabled sensor nodes periodically scan and identify available channels in the frequency spectrum. The network has one sink to collect the event readings in a timely and robust fashion.

Time is slotted in the cognitive radio sensor network operation. Time slots have two mini slots. The first one is for the spectrum sensing, and the second one is for data transmission and reception. The time slot for transmission is sufficient for packet transmission. One data symbol is transmitted in one time slot duration T_s . Hence, a node can transmit its packet if the channel is idle. Nodes can access the decided channel using CSMA/CA medium access protocol for wireless medium. Sensor nodes sense the spectrum bands without any error.

3.2.2 Traffic Model

The traffic in the CRSN is event-driven. An event in the monitoring area triggers the communication. The nodes in the network are idle at most of the time, however, they become active abruptly after the occurrence of an event. In our scenario, an event affecting the region with the event radius R is considered for the event model. The nodes within this radius sample the event and generate independent packets. These packets are conveyed to the sink in multi-hop manner in multi-channel environment. During the transmissions of the packets, some of them can not reach to the sink due to loss, hence they need to be transmitted again by the source. Primary user transmit data with probability p_t without any failure on any operating channel.

A packet generated by an event detecting node i is denoted by x_i . Event detecting nodes use geographical routing for the transmission of the data from the event to the sink. We exploit the broadcast nature of the CRSN nodes. The source symbols generated by the event detecting nodes are the data packets. A CRSN node sends its packet when the channel is idle without any collision. Symbol and packet are used interchangeably in this chapter.

The packets at the source nodes are directed to the sink. The information flow is always toward to the sink [24]. During this flow, communicating nodes contend for the medium at time slots reserved for communications. We assume that there is no collision for the contention.

The computation of data symbols is less energy consuming operation than the transmissions of data symbols. Hence, we use network coding for processing the received data symbols as explained in Section 3.3. In this operation, it is sufficient for the sink node to gather innovative packets whose number is the same with the event detecting nodes. This coding make the network more robust since the sink only needs gathering a number of innovative packets.

Encoding is performed by some source nodes which are at the intersection of the different source flows. Intermediate nodes between event and sink also perform encoding operations. Decoding is only performed by the sink node.

3.3 Network Coding

In this section, we present brief information about network coding in the literature. Network coding is a new technique for information flow in networks [41]. Routers in the wireline networks are allowed to mix the incoming packets and generate new set of encoded packets. If sufficient number of encoded packets arrive at the destination, destination nodes decode these packets according to Gaussian elimination method to achieve minimum-cut max-flow capacity in multicast networks [41]. In [42], the authors presented an algebraic framework for network coding to achieve capacity in networks. Furthermore, the authors in [43] proposes linear codes by decreasing encoding and decoding complexity by achieving capacity. Ho *et al.* proposes the coefficients of *native* packets in encoded packets to be random over a finite field [44]. This randomness offers the benefit of decentralized operation. Success probabilities of random linear network coding is also investigated and as the field size increases, the probability of the encoded packet becoming an *innovative* packet

increases since the random numbers are generated from a greater set.

Network coding has been performed in wireless networks recently. The broadcast nature of the wireless communications provide benefits for network coding since nodes opportunistically listen the packets of neighbors to generate encoded packets. Katti *et al.* use opportunistic listening in wireless routers and present COPE architecture for wireless mesh networks. Mixing the incoming packets increases the information content of the encoded packets. COPE is one of the first practical implementation of the network coding for wireless networks. Furthermore, there has been efforts to minimize the energy-per-bit by utilizing network coding in wireless networks. In [47], authors investigate the network coding advantage over routing and study the minimum energy required for multicast by linear programming. Network coding is also used in content distribution [48, 49], broadcasting [50, 51] and unicast [52] applications for different types of wireless networks.

Network coding has been recently implemented in sensor networks [53, 54, 55]. In these works, network coding is used for energy efficiency and reliability in sensor networks. Furthermore, there are not enough research on network coding in cognitive radio networks. In [56], network coding technique is implemented to improve the throughput of the secondary networks with minimum energy per bit consideration under interference and signal to interference plus noise constraint.

3.3.1 Practical Network Coding

We apply the network coding technique proposed by Chou *et al.* [57]. The authors consider the real packet networks where packets are subject to random delays and losses. They propose a network coding scheme that is not requiring a centralized knowledge about the network. This property perfectly matches the decentralized CRSN regime.

The network can be represented by directed graph $\mathcal{G} = (\mathcal{V}, \mathcal{E})$ where \mathcal{V} is the set of nodes or vertices and \mathcal{E} is the set of edges that interconnect some of these nodes. An edge from node u to node v can be shown as $e = (u, v)$, and $v = in(e)$ and $u = out(e)$. The edges directed to node v carry symbols to combined. If an outgoing symbol from an edge e' is denoted by $y(e')$, then the encoded symbol for node v is

$$y(e) = \sum_{e': out(e')=v} m_e(e')y(e') \quad (3.1)$$

where $m(e')$ is the encoding coefficient of the input symbol $y(e')$. In vector form, the local encoding vector can be represented as $\mathbf{m}(e) = [m_e(e')]_{e':out(e')=v}$.

The symbol on any edge is a linear combination of h source symbols. Hence, the global encoding vector along an edge e is denoted by

$$y(e) = \sum_{e':out(e')=v} m_e(e')y(e') = \sum_{i=1}^h g_i x_i \quad (3.2)$$

. The total received symbol coefficient matrix R can be represented as

$$R = \begin{bmatrix} g_{11} & \cdots & g_{1h} \\ \vdots & \ddots & \vdots \\ g_{h1} & \cdots & g_{hh} \end{bmatrix} \begin{bmatrix} x_1 \\ \vdots \\ x_N \end{bmatrix} = G\mathbf{x}. \quad (3.3)$$

If the sink receives h independent encoded symbols, the matrix G is invertible. It decodes the information successfully by taking the inverse of G . The decoded symbols can be found as $\mathbf{x} = G^{-1}R$.

The encoding coefficients are generated randomly from a finite field. If the field size is sufficient enough, the sink can recover the information with high probability. Hence, the field size is important for decodability.

In the packet format, the encoded packet must contain the coefficients of each source symbols to specify the content of the packet. However, this means simply an overhead. For example, if the number of source symbol h is 10, and the field size is 2^8 , then the overhead is 10 bytes. Since the packet size in sensor networks is small, the overhead may be excessive and it may deteriorate the energy efficiency.

In our scenario, an event triggers h nodes to create packets which are independent of each other. All h sessions are directed to same destination, i.e., the sink. Hence, our scenario is an application of inter-session network coding. The communication is the union of multiple unicast flows having the same destination.

3.4 Performance Evaluation

In this section, we present the simulation results on the performance of network coding in CRSN. We develop a simulation environment using MATLAB to evaluate the performance. We investigate

the performance of CRSN with and without network coding.

3.4.1 Simulation Environment

In our setting, a node having a packet transmits it to the one-hop neighbors closer than itself to the sink. A channel is randomly selected from the vacant channel set of the transmitter. In our simulation setup, secondary nodes are randomly distributed in a 50 m x 50 m area. Also, 20 primary users are randomly distributed in the area. There are 5 channels in the system, and a channel is assigned randomly to each primary user.

3.4.2 Energy-Efficiency

In this subsection, we investigate the effect of network coding on energy consumption. The number of sources, h , changes according to the event radius R . The effect is investigated according to the changes in the transmission range, the event radius, and the distance between event and sink.

In Fig. 3.2, we investigate the effect of cognitive radio transmission range on total energy consumption with and without network coding. An event with event radius 10 m is generated at (25 m, 25 m). In network operation, event detecting nodes send their messages to the one-hop neighbors closer to the sink over randomly selected vacant channel. Some messages are not received due to packet erasure probability. As seen in Fig. 3.2, as we increase the transmission range, total energy consumption increases. The increase in the range results in more nodes to hear about the transmission. Hence, nodes have to transmit more packet. Network coding has less total energy consumption since it benefits from the encoding operation such that a node can combine different flows into one flow which results in less energy consumption.

In Fig. 3.3, we investigate the effect of event radius, R . The event is generated at (25 m, 25 m). As the event radius increases, more nodes become source nodes. This increase is the cause of overhead since more bits are reserved to represent the coefficients. In Fig. 3.3, greater event radius results in more source packets and more packet transmissions which causes increase in energy consumption. If the event radius is less than $R = 7$ m, the encoding overhead causes more energy consumption, therefore, total energy consumption in network coding scenario is greater than the scenario without network coding. As event radius increases, the increase in source message results

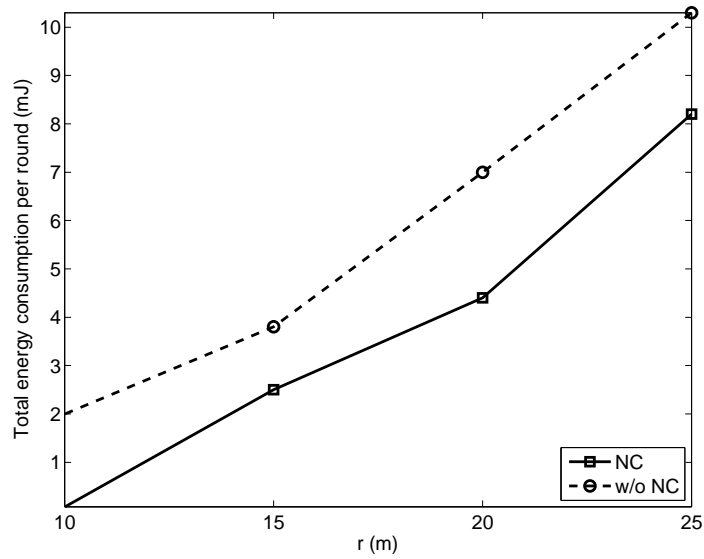


Figure 3.2: Total energy consumption (mJ) with respect to r (m) with and without network coding.

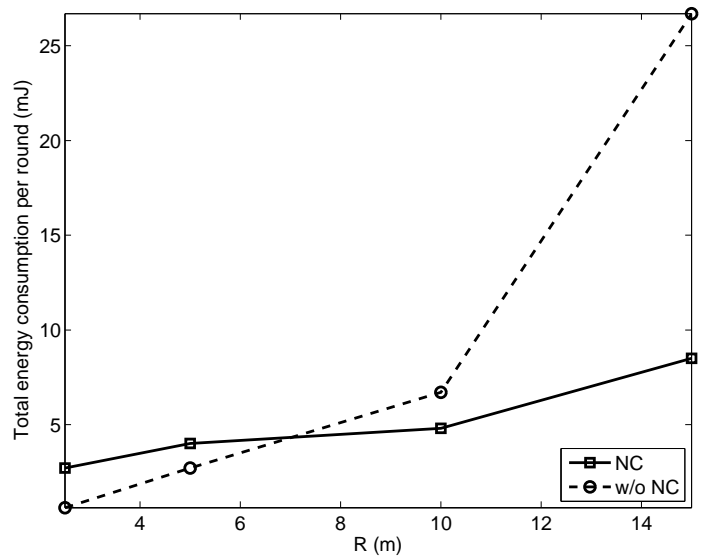


Figure 3.3: Total energy consumption (mJ) with respect to R (m) with and without network coding.

in more message transmission beyond the network coding overhead. This increase causes increase in overhead, however, there are more transmission effort for data delivery to recover all the source symbols. Hence, more energy is consumed for the scenario without network coding for event radius greater than 7 m. Since network coding decreases the transmission by combining packets, there is less energy consumption when using network coding as compared to the case without employing network coding.

In Fig. 3.4, event radius is 10 m and transmission range r is 20 m. As the event to sink distance increases, more nodes join the communication process. Hence, the total energy consumption increases. With network coding, only h independent messages are necessary to recover source messages. On the other hand, without network coding some incoming packets are the same and the nodes transmit duplicate messages unnecessarily. This redundancy causes more energy expenditure.

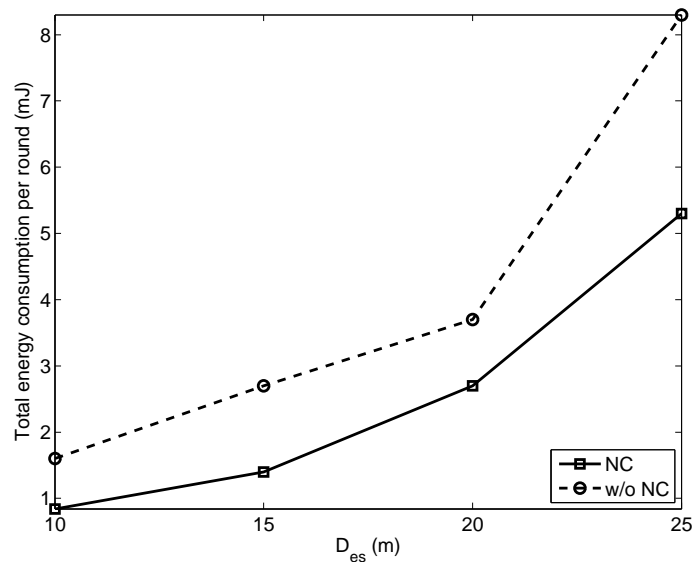


Figure 3.4: Total energy consumption (mJ) with respect to respect to D_{es} (m) with and without network coding.

3.4.3 Packet delivery ratio

In sensor networks, high packet delivery ratio is highly desirable with the limited energy resource. Hence, network coding effect on delivery ratio is investigated with respect to transmission range. In this simulation setup, the packet erasure probability of any link for all channel is set to be 0.3. Network coding provides more reliable communication in average since it is sufficient to recover h number of linearly independent packets. However, in some cases, if the sink does not receive the sufficient packets, it cannot recover the source messages and the reliability becomes zero. In our simulation settings, since the channel erasure probability is 0.3, we do not observe this all-or-nothing effect much and the source symbols are mostly recovered. The effect is observed only in smaller CR transmission range cases. As transmission range of CR increases, more packets delivered to the sink. Hence, the packet delivery ratio increases. Furthermore, as the transmission range increases, more coding opportunity occurs and more packets are mixed at the encoding nodes. This increases the linear independency among the encoded packets and it has a positive effect on reliability.

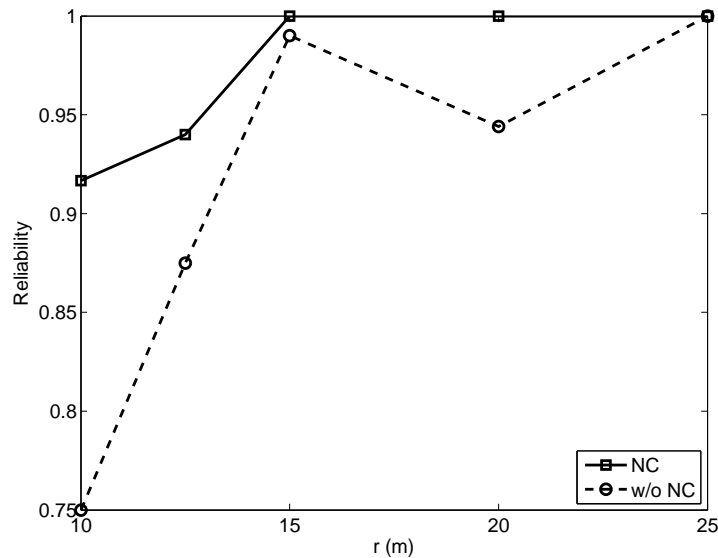


Figure 3.5: Packet delivery ratio per event with respect to transmission range.

Chapter 4

ON THE MAXIMUM COVERAGE AREA OF WIRELESS NETWORKED CONTROL SYSTEMS WITH MAXIMUM COST-EFFICIENCY UNDER STABILITY CONSTRAINT

The integration of wireless communication and control systems revealed wireless networked control systems (WNCSs). One fundamental problem in WNCSs is to have a wide coverage area. For the first time in the literature, we address this problem and we obtain the maximum coverage area by solving an optimization problem. In this chapter, we consider a WNCS where the output sensor measurements are transmitted over separate multi-hop wireless ad-hoc sensor subnetworks. We employ both homogeneous and heterogeneous multi-hop wireless ad-hoc sensor network models. The observation process is divided into N parts and the system state is estimated using the Kalman filter and we present the critical arrival probability for a sensor measurement packet such that if the packet arrival probability is larger than the critical value, it is guaranteed that the expected state estimation error covariance is bounded, and hence the WNCS is stable. We find the optimum hop-diameter of a multi-hop wireless ad-hoc subnetwork having maximum cost-efficiency under the constraint of the stability of the WNCS. Furthermore, under this constraint, we derive the maximum total coverage area of both the homogeneous and heterogeneous wireless ad-hoc sensor subnetworks with maximum cost-efficiency. The numerical analyses show that the maximum total coverage area can be increased by appropriately adjusting the number of sensors, the successful packet transmission probability between relay nodes, the transmission range of network nodes, and the eigenvalues of the system matrix.

4.1 Introduction

Recent developments on micro sensor integrated systems have enabled combination of communication and control systems. This integration revealed networked control systems (NCSs) where

the communication system enables the sensor observation delivery [59, 60]. The control system components such as sensors, actuators and plants with wireless communication capabilities constitute a wireless networked control system (WNCS). The observations of the sensors deployed over a wide area are fed to the WNCS through a wireless network. The WNCSs have a wide application area such as smart grid, automatic management and navigation systems [61].

For the WNCS applications requiring large coverage areas, e.g., space and terrestrial exploration, navigation systems, the maximum achievable area of the wireless network which ensures the stability of the WNCS is crucial. To the best of our knowledge, no attempt has yet been made to find the maximum coverage area of the wireless network under the stability of the WNCS constraint. For the first time in the literature, we address this problem and obtain the solution by solving an optimization problem [62]. Although in [63, 64], the authors investigate the maximum coverage area problem for wireless networks, they do not consider the stability of a WNCS which utilizes these wireless networks. In this chapter, we find the maximum coverage area of a wireless network having maximum cost-efficiency by considering the stability of the WNCS.

In our scenario, wireless sensor nodes are employed to observe the system behavior. We consider that the sensor measurements are transmitted to the controller over multi-hop wireless ad-hoc sensor networks. We employ both a homogeneous and a heterogeneous multi-hop wireless ad-hoc sensor network models. In the homogeneous network, each node is able to communicate with each other. However, in the heterogeneous network, cognitive radio sensor networks (secondary networks) coexists with licensed networks (primary networks) and the secondary network nodes cannot communicate with the primary network nodes. Cognitive radio sensor networks enable the unlicensed secondary users (SUs) to utilize the spectrum holes unoccupied by the licensed primary users (PUs) so that the spectrum resource utilization can be significantly increased [65]. Furthermore, two key properties of the multi-hop wireless ad-hoc networks are that they can be employed in a fast and easy way and very large coverage areas can be formed by means of their multi-hop property. However, measurement packets may be lost due to the unreliable wireless channel characteristics caused by the noise, collision, and congestion. Since the WNCSs rely on the observations of the sensors to estimate the state of the system, any loss of the sensor measurements degrades the stability of the WNCS.

We use the Kalman filter for the state estimation of the system. The Kalman filtering is a well investigated technique in control theory [66, 67]. In the classical sense, the Kalman filter uses all the observation data provided by the sensors for the state estimation. However, for the WNCSs, the observations may be lost due to wireless channel conditions as stated above. In [66], the Kalman filter is studied when the observations are intermittent; nevertheless, the authors do not consider statistical convergence behavior. In [67], the authors investigate the state estimation process, in which the sensor measurements are received or lost completely in a stochastic manner, and they show that if the probability of arrival of an observation is above a threshold, the expectation of the state estimation error covariance is bounded. In [68], the authors consider two sensors, and the measurement of each sensor is independently received or lost by the Kalman filter.

We present the general case of the system presented in [68]. The observation process is divided into N parts and each part is independently and randomly received or lost by the Kalman filter. Thus, we consider N separate multi-hop wireless ad-hoc subnetworks for our scenario and each subnetwork includes sensor nodes. Based on the derivations presented in [68], we derive the critical arrival probability for the measurement of each sensor such that if the arrival probability of a sensor measurement is larger than the critical value, it is guaranteed that the expectation of the state estimation covariance is bounded and the system is stable; otherwise it is not stable.

The packet arrival probability decreases as the number of hops during the packet transmission increases. The maximum hop number of the shortest paths between any two node pairs in the network is the hop-diameter of the network. We show that there exists a critical hop-diameter of a subnetwork such that if the hop-diameter of the subnetwork is less than the critical hop-diameter, the WNCS is stable. Another significant parameter for the WNCS is the cost-efficiency of the multi-hop wireless network. Based on the solution of an optimization problem, we find both the optimum hop-diameter and the maximum coverage area of the multi-hop wireless ad-hoc networks having maximum cost-efficiency under the constraint of the stability of the WNCS.

The chapter is organized as follows. In Section 4.2, we describe the Kalman filtering with partial observation losses. In Section 4.3, we present both the homogeneous and heterogeneous multi-hop wireless ad-hoc sensor network models and investigate the connectivity of these networks. In Section 4.4, we derive the maximum coverage area of the homogeneous and heterogeneous multi-

hop wireless ad-hoc sensor networks having maximum cost efficiency under the constraint of the stability of the WNCS. In Section 4.5, we present the numerical analysis of both optimum hop-diameter and maximum coverage area of multi-hop wireless ad-hoc sensor networks.

4.2 Kalman Filtering with Partial Observation Losses

In a WNCS, the Kalman filter gathers sensor measurements from distinct sensors and each sensor node encodes its own observation into a single packet. However, some of the packets might be lost during the wireless data transmission. In [68], the authors present a state estimation process with partial observation losses considering that the observation process is divided into two parts which are transmitted over different wireless channels by two different sensor nodes. In this section, we present a general state estimation process, i.e., the observation process is divided into N parts, with partial observation losses using the Kalman filter. In other words, the Kalman filter uses the output observations of N independent sensors.

We consider a general multiple-input multiple-output (MIMO) discrete time linear time-invariant system which is described by the following system equations

$$\begin{aligned} \mathbf{x}_{t+1} &= A\mathbf{x}_t + \mathbf{w}_t, \\ \begin{bmatrix} \mathbf{y}_{1,t} \\ \vdots \\ \mathbf{y}_{N,t} \end{bmatrix} &= \begin{bmatrix} C_1 \\ \vdots \\ C_N \end{bmatrix} \mathbf{x}_t + \begin{bmatrix} \mathbf{v}_{1,t} \\ \vdots \\ \mathbf{v}_{N,t} \end{bmatrix} \end{aligned} \quad (4.1)$$

where $\mathbf{x}_t \in \mathcal{R}^n$ is the system state vector, $\mathbf{w}_t \in \mathcal{R}^n$ is the system disturbance vector, $A \in \mathcal{R}^{n \times n}$ is the system matrix, $\mathbf{y}_{1,t} \in \mathcal{R}^{m_1}$, $\mathbf{y}_{2,t} \in \mathcal{R}^{m_2}$, \dots , $\mathbf{y}_{N,t} \in \mathcal{R}^{m_N}$ are sensor measurement output vectors, $\mathbf{v}_{1,t} \in \mathcal{R}^{m_1}$, $\mathbf{v}_{2,t} \in \mathcal{R}^{m_2}$, \dots , $\mathbf{v}_{N,t} \in \mathcal{R}^{m_N}$ are the measurement noise vectors, and $C_1 \in \mathcal{R}^{m_1 \times n}$, $C_2 \in \mathcal{R}^{m_2 \times n}$, \dots , $C_N \in \mathcal{R}^{m_N \times n}$ are the output matrices. The subscript t indicates the time index. Also note that the boldface symbols in this chapter represent vectors. We define $\mathbf{y}_t = [\mathbf{y}_{1,t}; \mathbf{y}_{2,t}; \dots; \mathbf{y}_{N,t}]$, $\mathbf{v}_t = [\mathbf{v}_{1,t}; \mathbf{v}_{2,t}; \dots; \mathbf{v}_{N,t}]$, and $C = [C_1; C_2; \dots; C_N]$. Both \mathbf{w}_t and \mathbf{v}_t are assumed to be Gaussian random vectors with zero mean and their covariance matrices are

$$Q \geq 0 \text{ and } R > 0, \text{ respectively. } R \text{ is defined by } R = \begin{bmatrix} R_{11} & \dots & R_{1N} \\ \vdots & \ddots & \vdots \\ R_{N1} & \dots & R_{NN} \end{bmatrix} \text{ where } R_{ij} = E[\mathbf{v}_{i,t} \mathbf{v}'_{j,t}].$$

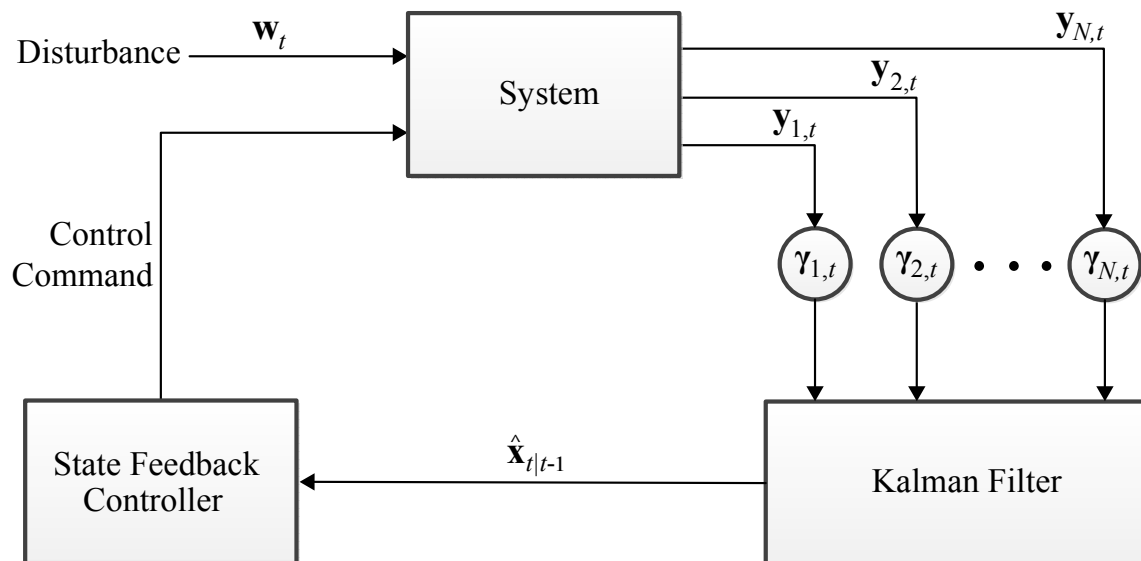


Figure 4.1: The block diagram of the WCSN.

Furthermore, we assume that the system (A, C) is observable; hence, the Kalman filter converges without sensor measurement losses.

The sensor measurement packets $\mathbf{y}_{1,t}, \mathbf{y}_{2,t}, \dots, \mathbf{y}_{N,t}$ are encoded independently and transmitted over different multi-hop wireless ad-hoc sensor subnetworks. We use random variable $\gamma_{i,t}$ which indicates whether the measurement packet of i^{th} sensor, $\mathbf{y}_{i,t}$, is correctly received during a given sample period. We assume $\gamma_{i,t}$ for $i = 1, 2, \dots, N$ are independent Bernoulli random variables with $\Pr\{\gamma_{i,t} = 1\} = \lambda_i$ and $\Pr\{\gamma_{i,t} = 0\} = 1 - \lambda_i$. That is, if $\gamma_{i,t} = 1$, then the measurement packet $\mathbf{y}_{i,t}$ is correctly received; otherwise, the packet is lost during the wireless data transmission. The arrival probabilities of the sensor measurements, i.e., λ_i for $i = 1, 2, \dots, N$, represent the percentage of the sensor measurement packets that are correctly received by the Kalman filter. Furthermore, λ_i for $i = 1, 2, \dots, N$ are proportional to the throughput of the communication link between the i^{th} sensor and the Kalman filter. Thus, the total network throughput of the multi-hop wireless ad-hoc network can be defined as $(\lambda_1, \lambda_2, \dots, \lambda_N)$, which depends on the channel gains, the network resource allocation, the network traffic, and the number of hops taken by a packet to reach the Kalman filter.

The block diagram of the WNCS for our scenario is shown in Fig. 4.1. Note that the observation

process is stochastic due to the random measurement losses during the packet transmission process. Furthermore, since we assume that $\gamma_{i,t}$ and $\gamma_{j,t'}$ for $i \neq j$ are independent for every t and t' , the sensor measurement packets $\mathbf{y}_{i,t}$ for $i = 1, 2, \dots, N$ can be independently lost or received. Therefore, the loss of a measurement packet is equivalent to the reception of a measurement having an infinite noise variance. Then, for the measurement noise vectors $\mathbf{v}_{i,t}$, we define the following conditional probability distribution function

$$f_{\mathbf{v}|\gamma}(\mathbf{v}_{i,t}|\gamma_{i,t}) \sim \begin{cases} \mathcal{N}(0, R_{ii}), & \text{if } \gamma_{i,t} = 1 \\ \mathcal{N}(0, \sigma_i^2 I), & \text{if } \gamma_{i,t} = 0. \end{cases} \quad (4.2)$$

Then, we take the limit as $\sigma_i^2 \rightarrow \infty$ to derive the Kalman filter equations in the case of random partial losses.

Let us define the vectors $\boldsymbol{\gamma}_t \triangleq [\gamma_{1,t}; \dots; \gamma_{N,t}]$, $\boldsymbol{\gamma}_0^t \triangleq \{\gamma_0, \dots, \gamma_t\}$, and $\mathbf{y}_0^t = \{\mathbf{y}_0, \dots, \mathbf{y}_N\}$. Then, we define

$$\begin{aligned} \hat{\mathbf{x}}_{t|t} &\triangleq \mathbb{E}[\mathbf{x}_t | \mathbf{y}_0^t, \boldsymbol{\gamma}_0^t], \\ P_{t|t} &\triangleq \mathbb{E}[(\mathbf{x}_t - \hat{\mathbf{x}}_{t|t})(\mathbf{x}_t - \hat{\mathbf{x}}_{t|t})' | \mathbf{y}_0^t, \boldsymbol{\gamma}_0^t], \\ \hat{\mathbf{x}}_{t+1|t} &\triangleq \mathbb{E}[\mathbf{x}_{t+1} | \mathbf{y}_0^t, \boldsymbol{\gamma}_0^t], \\ P_{t+1|t} &\triangleq \mathbb{E}[(\mathbf{x}_{t+1} - \hat{\mathbf{x}}_{t+1|t})(\mathbf{x}_{t+1} - \hat{\mathbf{x}}_{t+1|t})' | \mathbf{y}_0^t, \boldsymbol{\gamma}_0^t]. \end{aligned} \quad (4.3)$$

For the Kalman filter, the time update and the observation processes are independent. Hence, for our scenario, the time update process of the Kalman filter is formulated based on the classical Kalman filter as $\hat{\mathbf{x}}_{t+1|t} = A\hat{\mathbf{x}}_{t|t}$ and $P_{t+1|t} = AP_{t|t}A' + Q$. However, since the observation process is stochastic, the classical Kalman filter equations cannot be directly used for the measurement update process. Based on the results presented in [68], the state estimation error covariance $P_{t+1|t}$ can be expressed in terms of $P_{t|t-1}$ as $P_{t+1|t} = g(P_{t|t})$ where $g(X)$ is defined in (4.4), where $D_{i,j,\dots,k} = [C_i; C_j; \dots; C_k]$, $F_{i,j,\dots,k} = \text{Cov}[\mathbf{v}_{i,t}; \mathbf{v}_{j,t}; \dots; \mathbf{v}_{k,t}]$. Because of the stochastic nature of the Kalman filter updates, a unique deterministic state estimation error covariance cannot be obtained in the steady state. Therefore, we consider the statistical properties of the state estimation error covariance of the Kalman filter.

In [67], the authors investigate the state estimation process, in which the sensor measurement packet is received or lost completely, and they show the existence of a critical packet arrival prob-

$$\begin{aligned}
 g(X) &= AXA' + Q \\
 &- \gamma_{1,t}\gamma_{2,t}\dots\gamma_{N,t}AXC'(CXC' + R)^{-1}CXA' \\
 &- (1 - \gamma_{1,t})\gamma_{2,t}\dots\gamma_{N,t}AXD'_{2,\dots,N}(D_{2,\dots,N}XD'_{2,\dots,N} \\
 &\quad + F_{2,\dots,N})^{-1}D_{2,\dots,N}XA' \\
 &- \gamma_{1,t}(1 - \gamma_{2,t})\gamma_{3,t}\dots\gamma_{N,t}AXD'_{1,3,\dots,N}(D_{1,3,\dots,N}XD'_{1,3,\dots,N} \\
 &\quad + F_{1,3,\dots,N})^{-1}D_{1,3,\dots,N}XA' \\
 &- (1 - \gamma_{1,t})(1 - \gamma_{2,t})\gamma_{3,t}\dots\gamma_{N,t}AXD'_{3,\dots,N}(D_{3,\dots,N}XD'_{3,\dots,N} \\
 &\quad + F_{3,\dots,N})^{-1}D_{3,\dots,N}XA' \\
 &- \gamma_{1,t}\gamma_{2,t}(1 - \gamma_{3,t})\gamma_{4,t}\dots\gamma_{N,t}AXD'_{1,2,4,\dots,N}(D_{1,2,4,\dots,N}XD'_{1,2,4,\dots,N} \\
 &\quad + F_{1,2,4,\dots,N})^{-1}D_{1,2,4,\dots,N}XA' \\
 &\dots \\
 &- (1 - \gamma_{1,t})(1 - \gamma_{2,t})\dots(1 - \gamma_{N-1,t})\gamma_{N,t}AXD'_N(D_NXD'_N + F_N)^{-1}D_NXA'.
 \end{aligned} \tag{4.4}$$

ability λ^c such that $E[P_{t+1|t}]$ is bounded if $\lambda > \lambda^c$ and $E[P_{t+1|t}]$ becomes infinite as $t \rightarrow \infty$ if $\lambda < \lambda^c$. In addition, in [68], it is shown that for a state estimation process with random packet losses considering two measurement sensors, there is a critical packet arrival probability λ_1^c of the measurement of the first sensor given the packet arrival probability λ_2 of the second sensor. For the general case, based on the derivations and results given in [68], if (A, Q) is controllable and (A, C) is observable, for a fixed set of $(\lambda_1, \lambda_2, \dots, \lambda_{i-1}, \lambda_{i+1}, \dots, \lambda_N)$, if $\lambda_i \geq \lambda_i^c$, we can obtain positive semidefinite matrices $S \geq 0$ and $V \geq 0$ such that $0 \leq S \leq \lim_{t \rightarrow \infty} E[P_{t+1|t}] \leq V, \forall E[P_0] \geq 0$ where $S = (1 - \lambda_1)\dots(1 - \lambda_{N-1})ASA' + Q$ and $V = E[g(V)]$. Therefore, the WNCS stable, if the state estimation error covariance is bounded. Furthermore, we know that $P_{t+1|t}$ is bounded if and only if $E[P_{t+1|t}]$ is bounded. Thus, for a fixed set of $(\lambda_1, \lambda_2, \dots, \lambda_{i-1}, \lambda_{i+1}, \dots, \lambda_N)$, the WNCS is stable if and only if $\lambda_i \geq \lambda_i^c$.

If the output matrices C_1, C_2, \dots, C_N are square and invertible A has a single unstable eigenvalue, the upper and lower bounds for $\lim_{t \rightarrow \infty} E[P_{t+1|t}]$ coincide and the critical packet arrival

probability of the measurement packet of the i^{th} sensor becomes

$$\lambda_i^c = \max \left\{ 0, 1 - \frac{1}{\alpha^2(\lambda_1, \lambda_2, \dots, \lambda_{i-1}, \lambda_{i+1}, \dots, \lambda_N)} \right\} \quad (4.5)$$

where $\alpha = \max_i |\sigma_i|$ and σ_i is the i^{th} eigenvalue of A [68]. We discuss the appropriate selection of the set of $(\lambda_1, \lambda_2, \dots, \lambda_N)$ in Section 4.4 for a cost-efficient WNCS with the maximum coverage area under stability constraint.

4.3 Multi-Hop Wireless Ad-Hoc Sensor Network Models and Connectivity

For the WNCS, we employ multi-hop wireless ad-hoc sensor networks. The first advantage of multi-hop wireless ad-hoc sensor networks is that they can be employed in a fast and easy way, which is the reason why they are named “ad-hoc networks” [69]. The second advantage of this network model is that very large areas can be covered by means of the multi-hop property. However, since the wireless channels are unreliable, as the number of hops increases during the packet transmission, the packet arrival probability decreases.

In this chapter, we consider both a homogeneous and a heterogeneous multi-hop wireless ad-hoc sensor networks which are described in detail in the following subsections.

4.3.1 Homogeneous Network Model

We first consider a homogenous multi-hop wireless ad-hoc sensor network model. In a homogeneous network, each node is able to communicate with each other. For our scenario, we assume that there are N sensor nodes and each sensor transmits its measurement packet to the Kalman filter over a multi-hop wireless ad-hoc sensor subnetwork. In addition, it is assumed that the nodes in each sensor subnetwork are independently distributed according to a two dimensional homogeneous Poisson point process having a density ρ_0 . Each sensor subnetwork is considered as separate from each other. In Fig. 4.2, the multi-hop wireless ad-hoc sensor network model used in this chapter is shown where G_i denotes the i^{th} subnetwork including the i^{th} sensor node. We consider that the transmission ranges of all sensor and relay nodes are the same and denoted by r_0 . That is, if the distance between two nodes, r , satisfies $r \leq r_0$ condition, they are able to communicate directly via a wireless link.

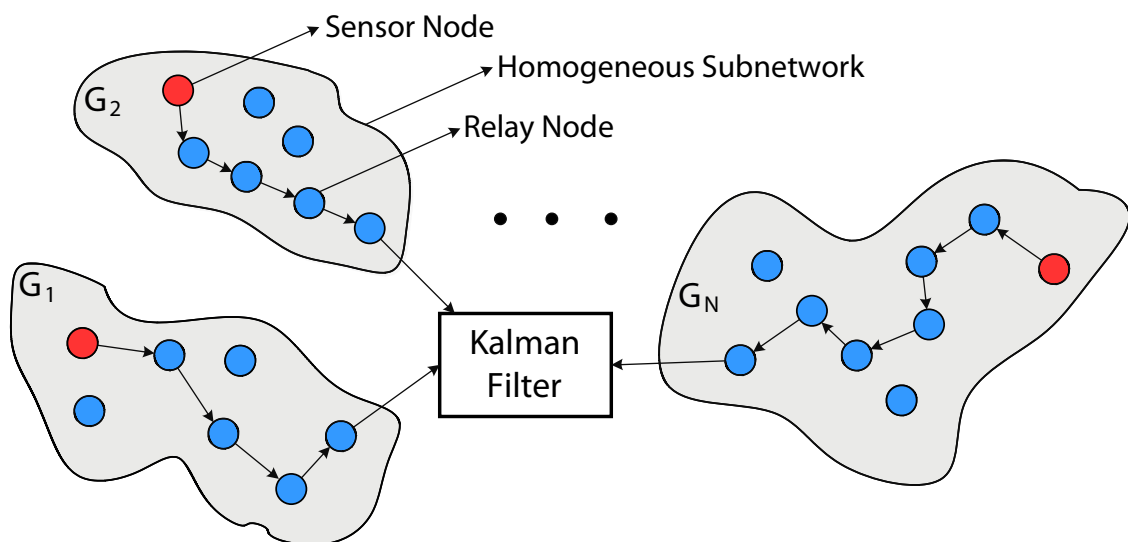


Figure 4.2: The model of the homogeneous multi-hop wireless ad-hoc subnetworks.

A very fundamental and significant property of multi-hop wireless ad-hoc sensor networks is the connectivity. To establish a fully connected ad-hoc sensor network, a wireless multi-hop path from each node to each other node must exist. According to the results in [69], assuming that the nodes in the network are distributed according to a two dimensional Poisson point process, there is a critical node density ρ_0^* such that if the node density of the network is larger than ρ_0^* , the network is connected with a certain probability. The critical node density ρ_0^* is given by

$$\rho_0^* = \frac{\ln \left[1 - P_1^{1/m_i} \right]^{-1}}{\pi r_0^2} \quad (4.6)$$

for $i = 1, 2, \dots, N$, where P_1 is the probability that a multi-hop wireless ad-hoc network is 1-connected, i.e., $P_1 = \Pr\{G_i \text{ is 1-connected}\}$, m_i is the total number of nodes in the subnetwork G_i , and r_0 is the transmission range of a node. A network is said to be 1-connected if for each pair of nodes, there exist at least 1 mutually independent link that connects them. Note that from (4.6), for a given number of nodes, if we set $P_1 = 1$, the node density of the network becomes infinite which is not realistic. However, if we set the probability that G_i is 1-connected as $P_1 = 0.99$, it can be said that the G_i subnetwork is almost surely connected. Therefore, in this chapter, we consider that the subnetwork G_i is 1-connected with probability $P_1 = 0.99$ and the subnetwork

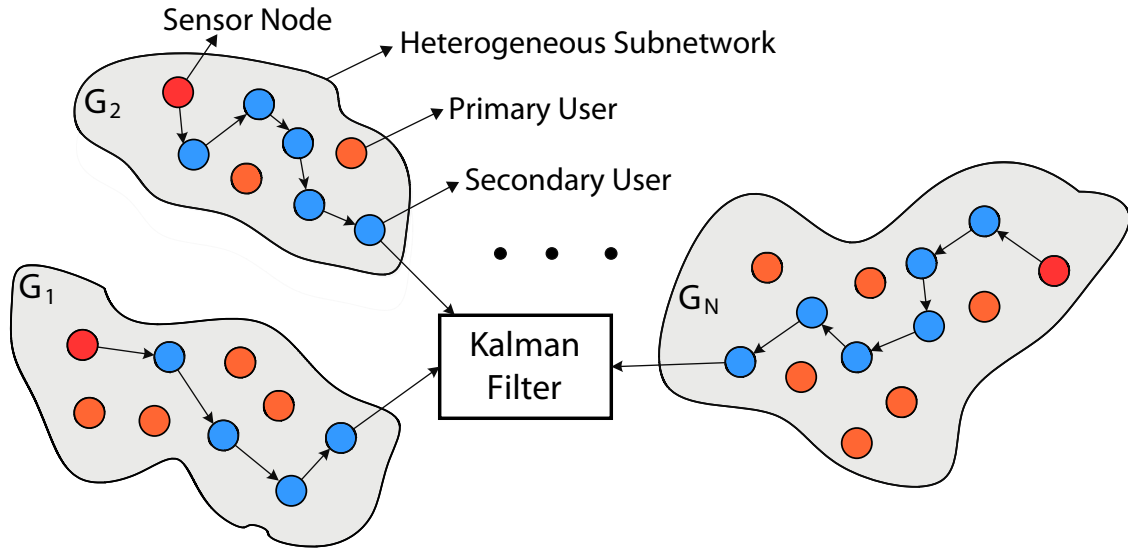


Figure 4.3: The model of the heterogeneous multi-hop wireless ad-hoc subnetworks.

G_i is almost surely connected.

4.3.2 Heterogeneous Network Model

Next, we consider a heterogeneous multi-hop wireless ad-hoc sensor network model in which cognitive radio ad-hoc networks (secondary networks) coexists with licensed networks (primary networks). In such a heterogeneous network, the secondary network nodes, i.e., Secondary Users (SUs), cannot communicate with the primary network nodes, i.e., Primary Users (PUs). Cognitive radio ad-hoc networks enable the unlicensed secondary users to utilize the spectrum holes unoccupied by the licensed primary users so that the limited spectrum resource is more efficiently used [65]. For the analysis presented in this part, we assume that the sensor measurements are transmitted to the Kalman filter over the cognitive radio multi-hop wireless ad-hoc sensor subnetworks.

In this part, we assume that the primary users are distributed according to two dimensional homogeneous Poisson point process having a density ρ_p . We consider that the transmission ranges of all primary network nodes are the same and denoted by r_p . Furthermore, we assume that the secondary network nodes, i.e., cognitive radio network nodes, are distributed according to two di-

dimensional homogeneous Poisson point process having a density ρ_s . The transmission ranges of all secondary network nodes are the same and denoted by r_s . The connectivity of cognitive radio networks is more troublesome than the connectivity of homogeneous networks. That is, the secondary cognitive radio network is connected if each node pair SU_i and SU_j in the cognitive radio network satisfies the following conditions:

1. The distance between SU_i and SU_j , r , satisfies $r \leq r_s$ condition.
2. Both SU_i and SU_j are outside the transmission range r_p of every active sender in the primary network.
3. There is no active primary network receiver in the transmission range r_s of SU_i and SU_j .

The first condition guarantees that there is a direct wireless link between the SUs. The second condition ensures that the active PUs do not generate any interference to SU_i and SU_j so that two SUs can utilize an available channel to communicate with each other. The third condition enables that the communications between two SUs does not interfered by the active PU receivers. In Fig. 4.3, the heterogeneous multi-hop wireless ad-hoc network model used in this chapter is shown where G_i denotes the i^{th} cognitive radio subnetwork including the i^{th} sensor node.

In [70], the authors show that there exists a critical node density ρ_s^* such that if the node density of the secondary network is larger than ρ_s^* , the secondary network percolates at all time, i.e., there exists always an infinite connected component in the secondary network under the time-varying spectrum availability. To guarantee the connectivity of the secondary network, we use the upper bound of the critical node density which is given by [70]

$$\rho_s^* = \frac{5}{r_s^2} \ln \left[1 - \sqrt{(1 - (\sqrt{6}/3)^\Lambda) e^{(|R_e| + |R'_e|)\Pi_1 \rho_p}} \right]^{-1} \quad (4.7)$$

where

$$\begin{aligned}\Lambda &= (4Ld + 2d + 1) \times (4Ld + d) + (4Ld + d + 1) \times (4Ld + 2d) - 1 \\ |R_e| &= (2 + 2\lceil r_p/d \rceil) \times (1 + 2\lceil r_p/d \rceil) \times d^2 \\ |R'_e| &= (2 + 2\lceil r_s/d \rceil) \times (1 + 2\lceil r_s/d \rceil) \times d^2 \\ L &= \lceil \max\{r_p, r_s\}/d \rceil \\ d &= r_s/\sqrt{5}.\end{aligned}$$

We assume that each PU sender is associated with an independent and identically distributed (i.i.d.) alternating renewal process, denoted by $S_p(t)$, which alternates between two states: the ON state, during which the PU is active; and the OFF state, during which the PU is inactive. Π_1 in (4.7) is defined as $\Pi_1 = \Pr\{S_p(t) = 1\}$. That is, Π_1 can be considered as the expected activation rate of a PU.

In the next section, to maximize the coverage area of a WNCS, we assume that the node densities of the homogeneous and heterogeneous multi-hop wireless ad-hoc networks are the same as the critical node densities ρ_0^* and ρ_s^* , respectively.

4.4 Maximum Coverage Area of Cost-Efficient Networks Under Stability Constraint

In a multi-hop network, we can increase the coverage area by increasing the number of nodes in the network. However, if the coverage is enlarged with an increase in the number of nodes, the number of hops during the packet transmission between two distant nodes rises. Because of the unreliable wireless channels, an increase in the number of hops during the packet transmission decreases the packet arrival probability, and the WNCS might become unstable as discussed in Section II. Therefore, for a stable WNCS, the hop-diameter of the network becomes a critical parameter. In the chapter, the hop-diameter of the subnetwork G_i is denoted by d_i .

In this chapter, the successful packet transmission probability between two nodes, which are within the transmission range of each other, is assumed to be constant and the same for each transmission process in the network and it is denoted by β . Therefore, the probability that the i^{th} sensor measurement is correctly received by the Kalman filter, i.e., λ_i , can be expressed as

$$\lambda_i = \beta^{M_i}, \quad \text{for } i = 1, 2, \dots, N \quad (4.8)$$

where M_i is the number of hops taken by the packet transmitted by the i^{th} sensor until it reaches the Kalman filter. M_i depends on the routing protocol, network topology, and number of nodes in the network.

Let the critical packet arrival probability of the i^{th} sensor measurement be λ_i^c . Based on the definition of the hop-diameter of a network, the maximum number of hop taken by a measurement packet until it reaches the Kalman filter is less than or equal to the hop-diameter of the subnetwork. Then, using (4.8), the critical-hop diameter of i^{th} subnetwork is

$$d_i^c = \lfloor \ln(\lambda_i^c) / \ln(\beta) \rfloor. \quad (4.9)$$

That is, if the hop-diameter of the subnetwork G_i satisfies $d_i \leq d_i^c$ condition, it is guaranteed that the arrival probability of the packet transmitted by i^{th} sensor is larger than the critical arrival probability; hence, the WNCS is stable. However, if $d_i > d_i^c$, the stability of the system is not guaranteed. Since the hop-diameter depends on several factors such as topology, network size, node locations, sensor communication range, and node density, it is difficult to find an upper bound for the maximum number of nodes which ensures a given hop-diameter. Therefore, to guarantee the stability of the control system, one can use a lower bound for the maximum number of nodes in a subnetwork given as $m_i(\lambda_i^c) = d_i^c + 1$ where $m_i(\lambda_i^c)$ denotes the number of nodes which guarantees that the packet arrival probability is less than the critical value and the proof is straightforward.

If we consider only the stability criterion, for a given set of $(\lambda_1, \lambda_2, \dots, \lambda_{i-1}, \lambda_{i+1}, \dots, \lambda_N)$, as $\lambda_i^c \rightarrow 0$, $m_i(\lambda_i^c) \rightarrow \infty$, and hence the total coverage area of the i^{th} subnetwork becomes infinite. Indeed, it is irrational and cost-inefficient to place infinitely many nodes in a subnetwork including a sensor node whose critical packet arrival probability is 0. That is, a decrease in λ_i^c decreases the importance of the subnetwork G_i , and when $\lambda_i^c = 0$, the measurements of the i^{th} sensor in G_i become unnecessary for the WNCS. Thus, for the maximum coverage area of the multi-hop wireless network, it is not enough to consider only the stability of the WNCS. The cost-efficiency of the multi-hop wireless network should also be considered. In other words, a multi-hop wireless network for a stable WNCS might have infinite coverage area. However, such a multi-hop wireless network is cost-inefficient. As a result, the selection of a set of packet arrival probabilities of the sensor measurements, i.e., $(\lambda_1, \lambda_2, \dots, \lambda_N)$, affects the cost-efficiency of the multi-hop wireless ad-hoc network.

Since when $\lambda_i \rightarrow 0$, $m_i(\lambda_i^c) \rightarrow \infty$ and $\lambda_i m_i(\lambda_i) \rightarrow 0$, we can use $\lambda_i m_i(\lambda_i)$ as the efficiency of the i^{th} subnetwork. Therefore, to find a cost-efficient multi-hop wireless ad-hoc network, we define a cost-efficiency function as follows

$$f(\lambda_1, \dots, \lambda_N) = \lambda_1 m_1(\lambda_1) + \dots + \lambda_N m_N(\lambda_N) \quad (4.10)$$

where $m_i(\lambda_i)$ is the number of nodes in the subnetwork G_i which guarantees that the packet arrival probability is bounded above by λ_i and it is given by $m_i(\lambda_i) = \lceil \ln(\lambda_i) / \ln(\beta) \rceil + 1$. Note that the cost-efficiency function is the weighted sum of the number of nodes in the subnetworks.

$$\begin{aligned} & \underset{\lambda_1, \dots, \lambda_N}{\text{maximize}} && f(\lambda_1, \dots, \lambda_N) = \lambda_1 m_1(\lambda_1) + \lambda_2 m_2(\lambda_2) + \dots + \lambda_N m_N(\lambda_N) \\ & \text{subject to} && \lambda_i < \max \left\{ 0, 1 - \frac{1}{\alpha^2(1-\lambda_1) \dots (1-\lambda_{i-1})(1-\lambda_{i+1}) \dots (1-\lambda_{N-1})} \right\} \\ & && \text{for } i = 1, 2, \dots, N \end{aligned} \quad (4.11)$$

Using (4.5), the set of $(\lambda_1, \lambda_2, \dots, \lambda_N)$ which both maximizes $f(\lambda_1, \dots, \lambda_N)$ and ensures the stability of the WNCS can be found by solving the optimization problem in (4.11). The solution of (4.11) is given by

$$\lambda_i^{\text{opt}} = \max\{e^{-\ln(\beta)-1}, 1 - \alpha^{-2/N}\} \quad (4.12)$$

for $i = 1, 2, \dots, N$, where $(\lambda_1^{\text{opt}}, \lambda_2^{\text{opt}}, \dots, \lambda_N^{\text{opt}})$ denotes the optimum stable set having the maximum cost-efficiency. The solution given in (4.12) satisfies the stability constraint of the WNCS and maximizes the cost-efficiency of the multi-hop wireless ad-hoc subnetworks. Then, using the optimum set of packet arrival probabilities given in (4.12), the optimum hop-diameter of the i^{th} subnetwork having the maximum cost-efficiency is given by

$$d_i^{\text{opt}} = \left\lceil \frac{\ln(\max\{e^{-\ln(\beta)-1}, 1 - \alpha^{-2/N}\})}{\ln(\beta)} \right\rceil. \quad (4.13)$$

Furthermore, to guarantee the stability of the WNCS, we use the lower bound for the maximum number of nodes in G_i , denoted by $m_i(\lambda_i^{\text{opt}})$, and it is

$$m_i(\lambda_i^{\text{opt}}) = \left\lceil \frac{\ln(\max\{e^{-\ln(\beta)-1}, 1 - \alpha^{-2/N}\})}{\ln(\beta)} \right\rceil + 1 \quad (4.14)$$

for $i = 1, 2, \dots, N$. Based on the number of nodes in each subnetwork having maximum cost-efficiency under the stability constraint, we can derive the maximum coverage area of the WNCS.

To find the coverage area of the subnetworks for the number of nodes given in (4.14), we consider the connectivity of the subnetworks. Thus, to have the maximum coverage area for a given number of nodes, we assume that the node densities of the homogeneous and heterogeneous multi-hop wireless ad-hoc networks are the same as the critical node densities ρ_0^* in (4.6) and ρ_s^* in (4.7), respectively. Then, for a stable WNCS, the maximum coverage area of the subnetwork G_i , which is 1-connected and cost-efficient, is given by $S_i^{hm} = m_i(\lambda_i^{\text{opt}})/\rho_0^*$ and $S_i^{ht} = m_i(\lambda_i^{\text{opt}})/\rho_s^*$. Since the number of nodes found in (4.14) is the same for each subnetwork, the maximum total coverage area of the homogeneous subnetworks is given by

$$S_T^{hm} = \frac{Nm_i(\lambda_i^{\text{opt}})\pi r_0^2}{\ln \left[1 - P_1^{1/m_i(\lambda_i^{\text{opt}})} \right]^{-1}}. \quad (4.15)$$

The maximum total coverage area of the heterogeneous subnetworks is given by

$$S_T^{ht} = \frac{Nm_i(\lambda_i^{\text{opt}})r_s^2}{5 \ln \left[1 - \sqrt{(1 - (\sqrt{6}/3)^\Lambda)} e^{(|R_e| + |R'_e|)\Pi_1 \rho_p} \right]^{-1}}. \quad (4.16)$$

Both S_T^{hm} and S_T^{ht} depend on several networks parameters such as transmission range of the network nodes and number of sensor nodes. In the next section, we investigate the effect of several network parameters on both the maximum total coverage area of the networks and optimum hop-diameter of the subnetworks.

4.5 Numerical Analysis

In this section, we present the numerical analyses of both the optimum hop-diameter d_i^{opt} and the maximum total coverage area S^T of the homogeneous and heterogeneous subnetworks with respect to several system and network parameters. For the numerical analyses, we assume that the output matrices C_1, C_2, \dots, C_N are square and invertible. The numerical evaluations are conducted using MATLAB.

4.5.1 Optimum Hop-Diameter of Subnetworks

In the first part of the numerical analyses, we present the variation of the optimum hop-diameter of subnetworks, d_i^{opt} , given in (4.13) with respect to the number sensor nodes, N , the successful packet transmission probability between two nodes, β , and the eigenvalue of A having the maximum magnitude, α . Since we assume that the successful packet transmission probability between two nodes is the same for both the homogeneous and heterogeneous subnetworks, the optimum hop-diameter of the subnetworks are the same for both type of subnetworks.

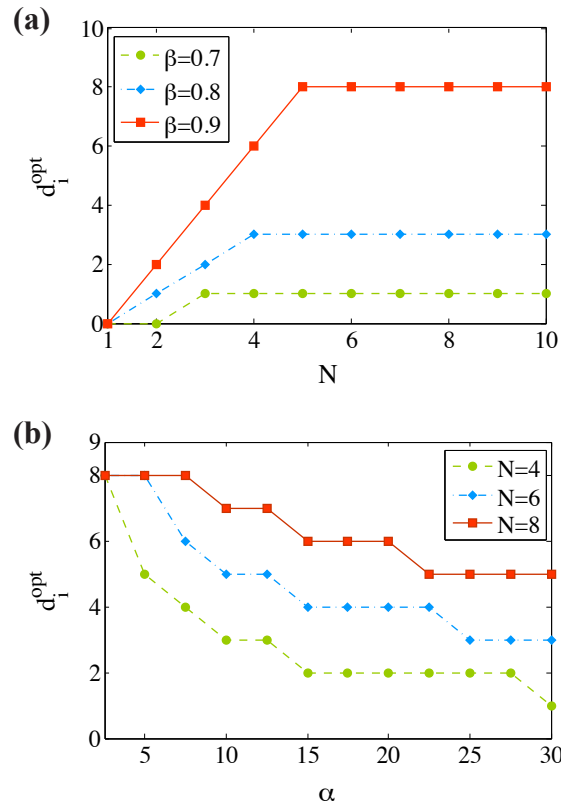


Figure 4.4: d_i^{opt} (a) with respect to N for different β values and (b) with respect to α for different N values.

In Fig. 4.4(a), d_i^{opt} with respect to the number of sensor nodes N employed for the WNCS with different β values is shown. d_i^{opt} increases with an increase in β which is an expected result. Note that $0 \leq \beta \leq 1$ and as $\beta \rightarrow 1$, $\ln(\beta) \rightarrow 0$, also the numerator in (4.13) is negative; hence, an increase

in β causes an increase in d_i^{opt} . As seen in Fig. 4.4(a), d_i^{opt} increases up to $N = 5$, then it becomes constant. If $N > -2 \ln(\alpha) / \ln(1 - e^{-\ln(\beta)-1})$, then $\max\{e^{-\ln(\beta)-1}, 1 - \alpha^{-2/N}\} = e^{-\ln(\beta)-1}$, and hence d_i^{opt} depends only on β . On the other hand, if $N < -2 \ln(\alpha) / \ln(1 - e^{-\ln(\beta)-1})$, then $\max\{e^{-\ln(\beta)-1}, 1 - \alpha^{-2/N}\} = 1 - \alpha^{-2/N}$; thus, d_i^{opt} depends on α and N , i.e., $d_i^{\text{opt}} = \ln(1 - \alpha^{-2/N}) / \ln(\beta)$. Obviously, d_i^{opt} decreases with an increase in α . For a fixed $\beta = 0.9$, the results seen in Fig. 4.4(b) show that d_i^{opt} decreases with an increase in α , which supports our inferences. It is also seen that d_i^{opt} can be increased with an increase in N .

4.5.2 Maximum Total Coverage Area of Homogeneous Network

In the second part of the numerical analyses, we investigate the maximum total coverage area of the homogeneous multi-hop wireless ad-hoc network model. In this section of the numerical analysis, we present the effect of r_0 , N , β , α on the maximum total coverage area of the homogeneous subnetworks, S_T^{hm} , given in (4.15). For the numerical analysis presented in this part, we consider that the subnetwork G_i is 1-connected with probability $P_1 = 0.99$.

In Fig. 4.5(a), for constant $N = 15$ and $\alpha = 4.0$, the variation of the maximum total coverage area S_T^{hm} with respect to r_0 is illustrated for different β values. S_T^{hm} is proportional with r_0^2 as seen in (4.15) and the quadratic dependence on r_0 can be seen in Fig. 4.5(a). In addition, the results show that an increase in β enlarges the total coverage area of the homogeneous subnetworks. From Section 4.5.1, we know that d_i^{opt} increases with an increase in β , and $m_i(\lambda_i^{\text{opt}}) = d_i^{\text{opt}} + 1$. Thus, from (4.15), it is obvious that S_T^{hm} becomes larger with an increase in d_i^{opt} .

In Fig. 4.5(b), for fixed $r_0 = 50\text{m}$ and $\alpha = 4.0$, the variation of S_T^{hm} with respect to the number of sensor nodes used for the WNCS for varying β values is demonstrated. According to the results, an increase in β enlarges the total coverage area of the homogeneous subnetworks because of the same reasons discussed above. Furthermore, S_T^{hm} becomes larger with an increase in the number of sensors N as shown in Fig. 4.5(b), which is an expected result because $S_T^{\text{hm}} = N S_i^{\text{hm}}$. Note also that, for each β value, S_T^{hm} increases in a quadratic trend up to $N = 5$; afterwards, it increases linearly with N . In Fig. 4.4(a), it is shown that up to $N = 5$, d_i^{opt} rises with an increase in N , which causes an increase in the maximum coverage area of a single homogeneous subnetwork S_i^{hm} and we know that $S_T^{\text{hm}} = N S_i^{\text{hm}}$. As a result, up to $N = 5$, S_T^{hm} increases quadratically. For $N > 5$,

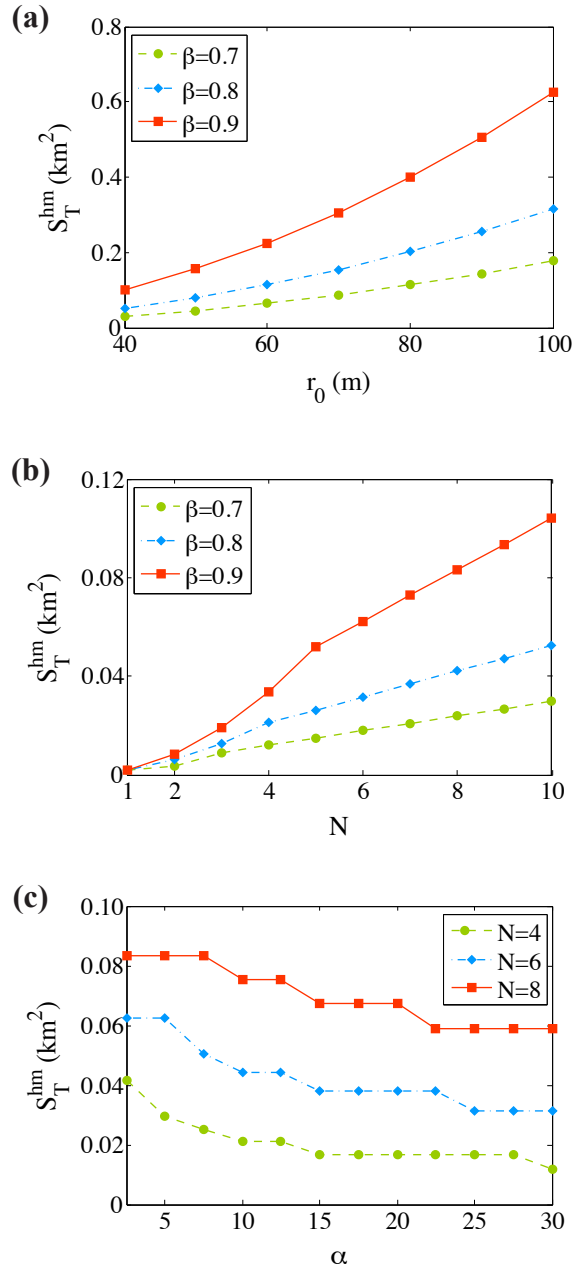


Figure 4.5: S_T with respect to (a) r_0 for different β values, (b) N for different β values, and (c) α for different N values.

since d_i^{opt} becomes constant, S_i^{hm} also becomes constant. Thus, for $N > 5$, S_T^{hm} increases linearly with N as seen in Fig. 4.5(b).

The effect of α , i.e., the eigenvalue of the system matrix A having the maximum magnitude, on the maximum total coverage area of the homogeneous multi-hop wireless subnetworks S_T^{hm} is shown in Fig. 4.5(c) for different N values. Here, we set $r_0 = 50\text{m}$ and $\beta = 0.9$. According to the results, an increase in α , causes a reduction in the maximum total coverage area S_T^{hm} . As we state previously, if $N > -2\ln(\alpha)/\ln(1 - e^{-\ln(\beta)-1})$, then $d_i^{\text{opt}} = \ln(1 - \alpha^{-2/N})/\ln(\beta)$. That is, for a given N , an increase in α decreases the optimum hop-diameter. Therefore, since $m_i(\lambda_i^{\text{opt}}) = d_i^{\text{opt}} + 1$, an increase in α also decreases S_T^{hm} , which can be seen in (4.15). Moreover, as illustrated in the figure, S_T^{hm} increases with an increase in N , which is discussed in detail above.

4.5.3 Maximum Total Coverage Area of Heterogeneous Network

In the last part of the numerical analyses, we consider the maximum total coverage area of the heterogeneous multi-hop wireless ad-hoc network model. In this part, we present the effect of r_s , r_p , N , β , α on the maximum total coverage area of the heterogeneous subnetworks, S_{ht}^T , given in (4.16). For the numerical analysis presented in this part, we consider that the secondary cognitive radio subnetwork G_i is connected. Furthermore, we set $\rho_p = 0.01\text{nodes/m}^2$.

In Fig. 4.6(a), for constant $r_p = 100\text{m}$, $\Pi_1 = 0.01$, $N = 15$ and $\alpha = 4.0$, the variation of the maximum total coverage area S_T^{ht} with respect to the transmission range of SUs, r_s , is illustrated for different β values. According to the results, S_T^{ht} increases with an increase in r_s which is an expected result. In addition, the results show that an increase in β enlarges the total coverage area of the subnetworks. From Section V-A, we know that d_i^{opt} increases with an increase in β , and $m_i(\lambda_i^{\text{opt}}) = d_i^{\text{opt}} + 1$. Thus, from (4.16), it is obvious that S_T^{ht} becomes larger with an increase in d_i^{opt} .

In Fig. 4.6(b), for constant $r_s = 50\text{m}$, $\Pi_1 = 0.01$, $N = 15$ and $\alpha = 4.0$, the variation of the maximum total coverage area S_T^{ht} with respect to the transmission range of PUs, r_p , is illustrated for different β values. According to the results, S_T^{ht} decreases with an increase in r_p . For connectivity of the secondary network, the PUs are required to be outside the transmission range of SUs as explained in Section 4.3.2. Thus, an increase in the transmission range of PUs decreases the number of connected nodes in the secondary network, which decreases the maximum total coverage area of the secondary subnetworks. In addition, the results show that an increase in β can significantly

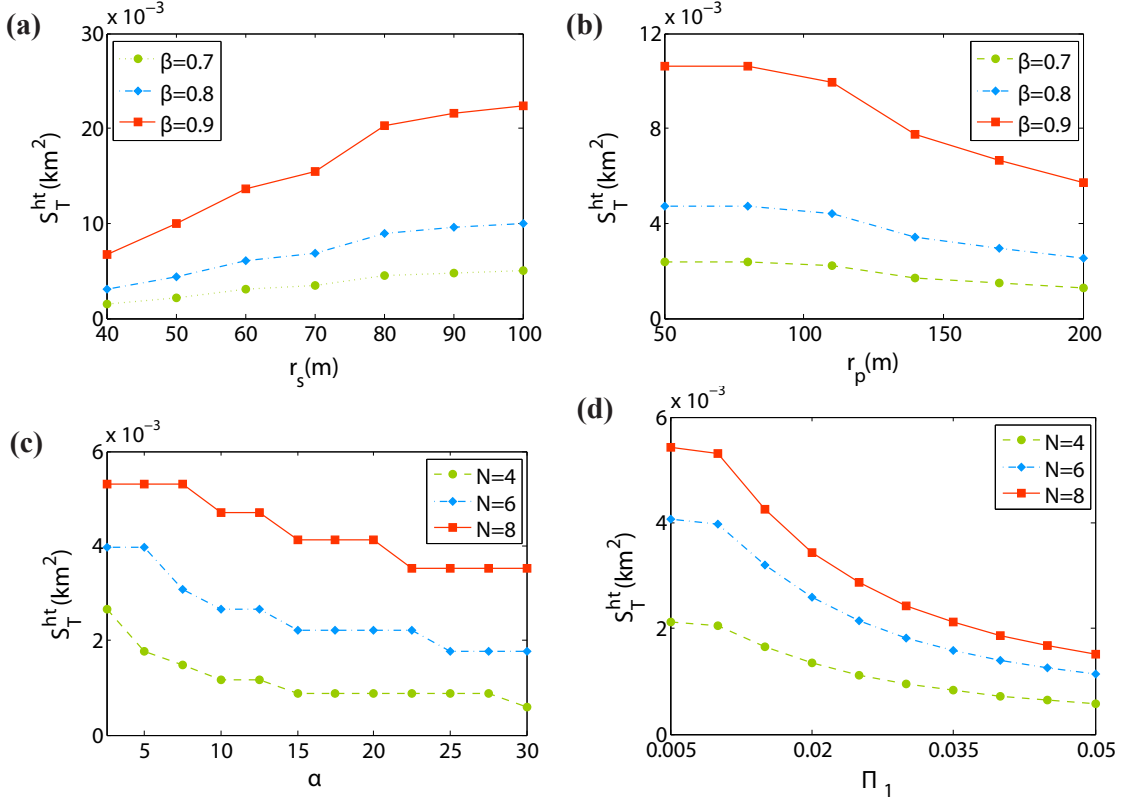


Figure 4.6: S_T^{ht} with respect to (a) r_s for different β values, (b) r_p for different β values, (c) α for different N values, and (d) Π_1 for different N values.

increase the total coverage area of the subnetworks as we stated above.

The effect of α , i.e., the eigenvalue of the system matrix A having the maximum magnitude, on the maximum total coverage area of the multi-hop wireless subnetworks S^T is shown in Fig. 4.6(c) for different N values. Here, we set $r_s = 50\text{m}$, $r_p = 100\text{m}$, $\Pi_1 = 0.01$, and $\beta = 0.9$. According to the results, an increase in α , causes a reduction in the maximum total coverage area S_T^{ht} . As we state in Section V-B, for a given N , an increase in α decreases the optimum hop-diameter. Therefore, since $m_i(\lambda_i^{\text{opt}}) = d_i^{\text{opt}} + 1$, an increase in α also decreases S_T^{ht} , which can be seen in (4.16). Moreover, as illustrated in the figure, S_T^{ht} increases with an increase in N , which is an expected result because $S_T^{ht} = N S_i^{ht}$.

In Fig. 4.6(d), the effect of Π_1 , i.e., the expected activation rate of PUs, on the maximum total

coverage area of the multi-hop wireless subnetworks S^T for different N values is demonstrated. For this analysis, we set $r_s = 50\text{m}$, $r_p = 50\text{m}$, $\alpha = 4.0$, and $\beta = 0.9$. According to the results, an increase in Π_1 , causes a reduction in the maximum total coverage area S_T^{ht} . As we state previously, activation of the PUs degrade the connectivity of SUs. That is, for the connectivity of the secondary network, the spectrum holes unoccupied by the licensed PUs are required. Therefore, an increase in the activation rate of the PUs decreases the number of connected nodes in the secondary network, which eventually decreases the maximum total coverage area of the secondary subnetworks. Moreover, as illustrated in the figure, S_T^{ht} increases with an increase in N , which is discussed in detail above.

Note that the maximum total coverage area of the secondary cognitive radio network is less than the maximum total coverage area of the homogeneous network by approximately one order of magnitude. For example, although for $r_0 = 40\text{m}$ and $r_s = 40\text{m}$, assuming rest of the parameters are the same, the maximum coverage of the homogeneous network is $S_T^{hm} = 99.8 \times 10^{-3}\text{km}^2$, the maximum coverage of the cognitive radio network is $S_T^{ht} = 6.8 \times 10^{-3}\text{km}^2$. Since the cognitive radio network nodes, i.e. SUs, utilize the spectrum holes unoccupied by the licensed PUs, the node density of the connected secondary network is higher than the node density of the connected homogeneous network. That is, the secondary network nodes are concentrated in narrow areas compared with the homogeneous network nodes. Therefore, the difference between the maximum total coverage areas of the homogeneous and cognitive radio networks is an expected result.

Chapter 5

CONCLUSIONS AND FUTURE RESEARCH DIRECTIONS

In this thesis, energy-efficient techniques such as clustering and network coding is applied to CRSN and coverage maximization is studied with cost efficiency constraint under stability constraint to realize CRSN. The following three topics have been investigated under this research and each of them is described in the following subsections:

1. Event-driven Spectrum-Aware Clustering
2. Network Coding
3. Coverage Maximization with Maximum Cost-Efficiency under Stability Constraint

5.1 Research Contributions

In this section, we summarize the contributions of each chapter and underline the important results.

5.1.1 Event-to-Sink Coordination in Cognitive Radio Sensor Networks

In this thesis, we present a clustering protocol for cognitive radio sensor networks to minimize the energy consumption. We aim to manage spectrum holes and establish energy-efficient communication by means of clustering. We propose on-the-fly coordination scheme for CRSN. The most important differences of our protocol than the others are that clustering is event-driven and in the corridor between event and sink. Furthermore, in our clustering protocol we establish a compromise between cluster size, common channels and two-hop neighbors that can be reachable by cluster-head through its members. Performance evaluation shows that ESAC is energy-efficient with a delay

caused by spontaneous cluster formation. It also forms more connected clusters avoiding isolated entities.

5.1.2 On the Effects of Network Coding in Cognitive Radio Sensor Networks

CRSN is an event-based system that the event-readings of sensor nodes are transmitted over multiple hops in spectrum-aware communication environment. Network coding is a novel technique that allows mixing of the incoming packet instead of simply relaying. In this section, we observe the effect of network coding in CRSN with respect to energy-efficiency and packet delivery ratio. According to our simulation results, CRSN may benefit from the advantages of network coding. In our network setup, we apply simple routing technique to observe the network coding effects, however, there is a need for network coding aware routing protocol by addressing the challenges of CRSN.

5.1.3 On the Maximum Coverage Area of Wireless Networked Control Systems with Maximum Cost-Efficiency under Stability Constraint

In this thesis, we investigate the maximum coverage area of homogeneous and heterogeneous multi-hop wireless ad-hoc sensor networks which are used for a WNCS with multiple sensors. We present the critical arrival probability for the measurement packet of a sensor such that if the probability of arrival of the packet is larger than the critical value, the state estimation error covariance is bounded and the system is stable. We find the optimum hop-diameter of the multi-hop wireless sensor subnetworks having maximum cost-efficiency under the constraint of the stability of the WNCS. Furthermore, we derive the maximum coverage area expressions of both homogeneous and heterogeneous networks having maximum cost-efficiency under the stability constraint of the WNCS.

The numerical analyses show that an increase in the successful packet transmission probability between two nodes and the number of sensors increases the optimum hop-diameter of the subnetworks, the maximum total coverage area of the both homogeneous and heterogeneous multi-hop wireless ad-hoc sensor networks. Furthermore, a decrease in the eigenvalue of the system matrix with maximum magnitude increases the optimum hop-diameter and the maximum total coverage

area of the multi-hop wireless ad-hoc networks. For homogenous network, increasing the transmission range of a node also increases the maximum coverage area of the network. On the other hand, in the heterogeneous network, increasing the transmission range of SUs and decreasing the transmission range and activation rate of PUs can significantly increase the maximum coverage area of the cognitive radio ad hoc network.

For the WNCS applications requiring wide coverage areas, e.g., space and terrestrial exploration and navigation systems, the maximum coverage area expressions can be used to construct a cost-efficient multi-hop network which ensures the stability of the control system. Moreover, using the analysis presented in this chapter, the maximum total coverage area can be increased by appropriately adjusting the number of sensors, the successful packet transmission probability between relay nodes, the transmission range of network nodes, and the eigenvalues of the system matrix.

5.2 Future Research Directions

The presentation of the event-driven spectrum-aware clustering brings a new perspective to CRSN. However, in our work, we assume single event cases. Hence, our protocol may be enhanced by studying multi-event cases. Furthermore, in our protocol we do not consider re-clustering case. Therefore, the enhanced solution must take into account temporal activities of spectrum opportunities in addition to the spatial variations of them.

Network coding has been applied to many wired and wireless networks thus far. On the other hand, there is not yet a study on network coding in CRSN. However, for the first time in the literature, we observed the effects of network coding in CRSN by simulation study. Due to the possible benefits of network coding, a new network coding-aware routing protocol may be presented by considering the challenges posed by cognitive radio and sensor network.

In this thesis, for the first time in the literature, we investigate the coverage maximization with maximum cost efficiency under stability constraint. However, there are open research issues for wireless network control systems consisting of cognitive radio sensor subnetworks. New routing and transport solutions may be developed by considering the cost-efficiency and stability challenges posed by wireless networked control systems.

REFERENCES

- [1] Spectrum Policy Task Force, "Spectrum Policy Task Force Report," *Federal Communications Commission ET Docket 02-135*, 2002.
- [2] I. F. Akyildiz, W. Y. Lee, M. C. Vuran, and S. Mohanty, "NeXt generation / dynamic spectrum access / cognitive radio wireless networks: A survey," *Computer Networks Journal (Elsevier)*, Sept. 2006.
- [3] S. Haykin, "Cognitive Radio: Brain-Empowered Wireless Communications," *IEEE Journal on Selected Areas in Communications*, vol. 23, no. 2, pp. 201-220, Feb. 2005.
- [4] O. B. Akan, O. Karli, and O. Ergul, "Cognitive radio sensor networks," *IEEE Network*, vol. 23, no. 4, pp. 34-40, July 2009.
- [5] X. Li, D. Wang, J. McNair, and J. Chen, "Residual energy aware channel assignment in cognitive radio sensor networks," in *Proc. IEEE WCNC 2011*, Quintana-roo, Mexico, 2011, pp. 398-403.
- [6] J. Han, W. Jeon, and D. Jeong, "Energy efficient channel management scheme for cognitive radio sensor networks," *IEEE Transactions on Vehicular Technology*, vol. 60, no. 4, pp. 1905-1909, May 2011.
- [7] A. O. Bicen, and O. B. Akan, "Reliability and congestion control in cognitive radio sensor networks," *Ad Hoc Network Journal (Elsevier)*, vol. 9, no. 7, pp. 1154-1164, Sep. 2011.
- [8] M. C. Oto, and O. B. Akan, "Energy-efficient packet size optimization for cognitive radio sensor networks," *IEEE Transactions on Wireless Communications*, vol. 11, no. 4, pp.1544-1553, April 2012.

-
- [9] B. Gulbahar, and O. B. Akan, "Information Theoretical Optimization Gains in Energy Adaptive Data Gathering and Relaying in Cognitive Radio Sensor Networks," *IEEE Transactions on Wireless Communications*, vol. 11, no. 5, pp. 1788-1796, May 2012.
- [10] Z. Liang, S. Feng, D. Zhao, and X. S. Shen, "Delay Performance Analysis for Supporting Real-Time Traffic in a Cognitive Radio Sensor Network," *IEEE Transactions on Wireless Communications*, vol. 10, no. 1, pp. 325-335, Jan. 2011.
- [11] C.r. Lin, and M. Gerla, "Adaptive clustering for mobile wireless networks," *IEEE Journal on Selected Areas in Communications*, vol. 15, no. 7, pp. 1265-1275, Sep. 1997.
- [12] S. Basagni, "Distributed clustering for ad hoc networks," in *Proc. of I-SPAN 1999*, Fremantle, Australia, 1999, pp. 310-315.
- [13] V. Kawadia, and P. Kumar, "Power control and clustering in ad hoc networks," in *Proc. of IEEE INFOCOM 2003*, San Francisco, CA, 2003.
- [14] M. Chatterjee, S. K. Das, and D. Turgut, "WCA: A Weighted Clustering Algorithm for Mobile Ad hoc Networks," *Journal of Cluster Computing (Special Issue on Mobile Ad hoc Networks)*, vol. 5, pp. 193-204, 2002.
- [15] S. Bandyopadhyay, and E. J. Coyle, "An energy efficient hierarchical clustering algorithm for wireless sensor networks," in *Proc. of INFOCOM 2003*, San Francisco, CA, 2003, pp. 1713-1723.
- [16] O. Younis, and S. Fahmy, "HEED: a hybrid, energy-efficient, distributed clustering approach for ad hoc sensor networks," *IEEE Transactions on Mobile Computing*, vol. 3, no. 4, pp. 366-379, Oct. 2004.
- [17] J.Y. Yu, and P.H.J. Chong, "A survey of clustering schemes for mobile ad hoc networks," *IEEE Communications Surveys and Tutorials*, vol. 7, no. 1, pp. 32-48, First Qtr. 2005.

-
- [18] A. A. Abbasi, and M. Younis, "A survey on clustering algorithms for wireless sensor networks," *Computer Communications (Elsevier)*, vol. 30, no. 14-15, pp. 2826-2841, Oct. 2007.
- [19] D. Baker, and A. Ephremides, "The Architectural Organization of a Mobile Radio Network via a Distributed Algorithm," *Communications, IEEE Transactions on*, vol. 29, no. 11, pp. 1694-1701, Nov 1981.
- [20] O. Younis, and S. Fahmy, "HEED: a hybrid, energy-efficient, distributed clustering approach for ad hoc sensor networks," *IEEE Transactions on Mobile Computing*, vol. 3, no. 4, pp. 366-379, Oct. 2004.
- [21] P. Ding, J. Holliday, and A. Celik, "Distributed energy efficient hierarchical clustering for wireless sensor networks," in *Proc. of IEEE DCOSS 2005*, Marina Del Rey, CA, 2005.
- [22] J. Zhao, H. Zheng, and G.-H. Yang, "Distributed Coordination in Dynamic Spectrum Allocation Networks," in *Proc. of IEEE DySPAN 2005*, Baltimore, MD, 2005.
- [23] T. Chen, H. Zhang, G.M. Maggio, and I. Chlamtac, "CogMesh: A Cluster-Based Cognitive Radio Network," in *Proc. of IEEE DySPAN 2007*, Dublin, Ireland, 2007, pp. 168-178.
- [24] M. Ozger, O.B. Akan, "Event-driven Spectrum-Aware Clustering in Cognitive Radio Sensor Networks," in *Proc. of IEEE INFOCOM 2013*, Turin, Italy, 2013, pp. 1483-1491.
- [25] M. Ozger, O.B. Akan, "Event-to-Sink Coordination in Cognitive Radio Sensor Networks," submitted to *IEEE/ACM Transactions on Networking*, 2013.
- [26] L. Lazos, S. Liu, and M. Krunz, "Spectrum opportunity-based control channel assignment in cognitive radio networks," in *Proc. of IEEE SECON 2009*, Piscataway, NJ, 2009, pp. 135-143.
- [27] M. Bradonjic, and L. Lazos, "Graph-based criteria for spectrum-aware clustering in cognitive radio networks," *Ad Hoc Networks (Elsevier)*, vol. 10, no. 1, pp. 75-94, Jan 2012.

- [28] K.E. Baddour, O. Ureten, and T. J. Willink, "Efficient Clustering of Cognitive Radio Networks Using Affinity Propagation," in *Proc. of IEEE ICCCN 2009*, San Francisco, CA, 2009.
- [29] D. Li, and J. Gross, "Robust Clustering of Ad-Hoc Cognitive Radio Networks under Opportunistic Spectrum Access," in *Proc. of IEEE ICC 2011*, Kyoto, Japan, 2011.
- [30] H. Zhang, Z. Zhang, H. Dai, R. Yin, and X. Chen, "Distributed spectrum-aware clustering in cognitive radio sensor networks," in *Proc. of IEEE GLOBECOM 2011*, Houston, TX, 2011.
- [31] A. Bereketli, and O.B. Akan, "Event-to-Sink Directed Clustering in Wireless Sensor Networks," in *Proc. of IEEE WCNC 2009*, Budapest, Hungary, 2009, pp. 1-6.
- [32] J. Jia, Q. Zhang, and X. Shen, "HC-MAC: A hardware-constrained cognitive MAC for efficient spectrum management," *IEEE Journal on Selected Areas in Communications*, vol. 26, no. 1, pp. 106-117, Jan. 2008.
- [33] H. Su, and X. Zhang, "Design and analysis of a multi-channel cognitive MAC protocol for dynamic access spectrum networks," in *Proc. of IEEE MILCOM 2008*, San Diego, CA, 2008.
- [34] W.-Y. Lee, I. F. Akyildiz, "Optimal spectrum sensing framework for cognitive radio networks," *IEEE Transactions on Wireless Communications*, vol. 7, no. 10, pp. 3845 -3857, Oct. 2008.
- [35] L. Yang, L. Cao, and H. Zheng, "Proactive channel access in dynamic spectrum networks," *Physical Communications*, vol. 1, no. 2, pp. 103-111, Jun. 2008.
- [36] L.-H. Yen, C. Yu, and Y.-M. Cheng, "Expected k-coverage in wireless sensor networks," *Ad Hoc Networks*, vol. 5(4), pp. 636-650, Sept. 2006.
- [37] G. A. Shah, and O. B. Akan, "CSMA-Based Bandwidth Estimation for Cognitive Radio Sensor Networks," in *Proc. of IEEE NMTS 2012*, Istanbul, Turkey, 2012, pp. 1-5.
- [38] W. Heinzelman, A. Chandrakasan, and H. Balakrishnan, "Energy Efficient Communication Protocol for Wireless Microsensor Networks," in *Proc. of HICSS 2000*, 2000.

- [39] Q. Zhao and B. M. Sadler, "A survey of dynamic spectrum access," *IEEE Signal Processing Magazine*, pp. 79-89, May 2007.
- [40] H. Zhang, Z. Zhang, and Y. Chau, "Distributed compressed wideband sensing in cognitive radio sensor networks," in *Proc. of IEEE INFOCOM Workshops 2011*, Shanghai, China, Apr. 2011.
- [41] R. Ahlswede, N. Cai, S.-Y. R. Li, and R. W. Yeung, "Network information flow," *IEEE Transactions on Information Theory*, vol. 46, pp. 1204-1216, July 2000.
- [42] R. Koetter, and M. Medard, "An algebraic approach to network coding," *IEEE/ACM Transactions on Networking*, vol. 11, pp. 782-795, Oct. 2003.
- [43] S. Y. R. Li, R. W. Yeung, and N. Cai, "Linear network coding," *IEEE Trans. Inform. Theory*, vol. 49, p. 371, Feb. 2003.
- [44] T. Ho, M. Medard, R. Koetter, D. R. Karger, M. Effros, J. Shi, and B. Leong, "A random linear network coding approach to multicast," *IEEE Transactions on Information Theory*, vol. 52, pp. 4413-4430, Oct. 2006.
- [45] J. S. Park, M. Gerla, D. S. Lun, Y. Yi, and M. Medard, "Codecast: A network-coding based ad hoc multicast protocol," *IEEE Wireless Comm. Magazine*, 2006.
- [46] S. Katti, H. Rahul., W. Hu, D. Katabi, M. Medard, and J. Crowcroft, "XORs in the Air: Practical Wireless Network Coding," in *Proceedings of ACM SIGCOMM 2006 Conference*, Pisa, Italy, Sep. 2006.
- [47] Y. Wu, P. A. Chou, and S.-Y. Kung, "Minimum-energy multicast in mobile ad hoc networks using network coding," *IEEE Transactions on Communications*, vol. 53, no. 11, pp. 1906-1918, Nov. 2005.

- [48] A. G. Dimakis, P. B. Godfrey, M. J. Wainwright, and K. Ramchandran, "Network Coding for distributed storage systems," *IEEE Proceedings of INFOCOM 2007*, Anchorage, Alaska, May 2007.
- [49] C. Gkantsidis and P. Rodriguez, "Network Coding for Large Scale Content Distribution," in *Proc. of IEEE INFOCOM 2005*, Miami, FL, USA, March 2005.
- [50] D. Nguyen, T. Nguyen, and B. Bose, "Wireless broadcasting using network coding," in *Proc. NetCod*, San Diego, CA, USA, January 2007.
- [51] J. Widmer, C. Fragouli, and J.-Y. Le Boudec, "Low-complexity energy-efficient broadcasting in wireless ad-hoc networks using network coding," in *Proc. Workshop on Network Coding, Theory, and Applications*, Apr. 2005.
- [52] S. Sengupta, S. Rayanchu, and S. Banerjee, "An analysis of wireless network coding for unicast sessions: The case for coding-aware routing," in *Proc. of IEEE INFOCOM 2007*, Anchorage, Alaska, May 2007.
- [53] I.-H. Hou, Y.-E. Tsai, T. Abdelzaher, and I. Gupta, "Adapcode: Adaptive network coding for code updates in wireless sensor networks," in *Proc. IEEE INFOCOM 2008*, Phoenix, AZ, USA, Apr. 2008.
- [54] L. Keller, E. Atsan, K. Argyraki, and C. Fragouli, "SenseCode: Network coding for reliable sensor networks," *EPFL Technical Report*, October 2009.
- [55] A. Kamra, J. Feldman, V. Misra and D. Rubenstein, "Growth codes: Maximizing sensor network data persistence," in *Proc. of ACM SIGCOMM 2006*, Pisa, Italy, Sep. 2006.
- [56] L. Geng, Y.-C. Liang, and F. Chin, "Network coding for wireless ad hoc cognitive radio networks," in *Proc. IEEE PIMRC 2007*, Athens, Greece, Sep. 2007, pp. 1-5.
- [57] P. A. Chou, Y. Wu, and K. Jain, "Practical network coding," in *Proc. 41st Annu. Allerton Conf. Communication, Control, and Computing*, Monticello, IL, Oct. 2003.

- [58] M. Ozger, and O.B. Akan, "On the Effects of Network Coding in Cognitive Radio Sensor Networks," submitted to *IEEE ICC 2014*, 2013.
- [59] Y. Halevi and A. Ray, "Integrated communication and control systems: Part I-Analysis," *J. Dynamic Syst., Measure. Contr.*, vol. 110, pp. 367-373, Dec. 1988.
- [60] M.S. Branicky, S.M. Phillips, and W. Zhang, "Stability of networked control systems: Explicit analysis of delay," in *Proc. Amer. Control Conf.*, Chicago, IL, June 2000, pp. 2352-2357.
- [61] A. Bemporad, M. Johansson, and M. Heemels, *Networked Control Systems*. Berlin, Germany, Springer, 2010.
- [62] D. Kilinc, M. Ozger, and O. B. Akan, "On the Maximum Coverage Area of Wireless Networked Control Systems under Stability and Cost-Efficiency Constraints," to appear in *Proc. IEEE GLOBECOM 2013*, Atlanta, GA, USA, December 2013.
- [63] C. F. Huang and Y. C. Tseng, "The coverage problem in a wireless sensor network," in *Proc. ACM Int. Conf. Wireless Sensor Networks and Applications (WSNA)*, 2003, pp. 115-121.
- [64] C. C. Tseng and K. C. Chen, "Power Efficient Topology Control in Wireless Ad Hoc Networks," in *Proc. IEEE Wireless Comm. and Networking Conf. (WCNC)*, 2004, pp. 610-615.
- [65] I. F. Akyildiz, W. Y. Lee, and K. Chowdhury, "CRAHNs: Cognitive radio ad hoc networks," *Ad Hoc Networks (Elsevier)*, vol. 7, no. 2, pp. 810-836, 2009.
- [66] T. Fortmann, Y. Bar-Shalom, M. Scheffe, and S. Gelfand, "Detection thresholds for tracking in clutter - a connection between estimation and signal processing," *IEEE Trans. Automat. Contr.*, vol. AC-30, pp. 221-228, Mar. 1985.
- [67] B. Sinopoli, L. Schenato, M. Franceschetti, K. Poola, M. I. Jordan, and S. S. Sastry, "Kalman filtering with intermittent observations," *IEEE Trans. Autom. Control*, vol. 49, no. 9, pp. 1453-1464, Sep. 2004.

-
- [68] X. Liu and A. Goldsmith, "Kalman filtering with partial observation losses," in *Proc. IEEE Conf. Decision and Control*, Bahamas, Dec. 2004, vol. 4, pp. 4180-4186.
- [69] C. Bettstetter, "On the Minimum Node Degree and Connectivity of A Wireless Multihop Network," in *Proc. ACM Int. Symp. Mobile Ad Hoc Networking and Computing*, Switzerland, June 2002, pp. 80-91.
- [70] P. Wang, I. F. Akyildiz, and A. M. Al-Dhelaan, "Dynamic connectivity of cognitive radio ad-hoc networks with time-varying spectral activity," in *Proc. IEEE GLOBECOM 2010*.
- [71] D. Kilinc, M. Ozger, and O. B. Akan, "On the Maximum Coverage Area of Wireless Networked Control Systems with Maximum Cost-Efficiency under Stability," submitted to *IEEE Transactions on Automatic Control*, 2013

CURRICULUM VITAE

MUSTAFA ÖZGER was born in Alanya on September 7, 1988. He graduated from Haydarpaşa Anatolian High School in 2006. He received his B.S. degree in Electrical and Electronics Engineering from Middle East Technical University (METU), Ankara, Turkey, in 2011. He received his M.S. degree under the supervision of Prof. Ozgur B. Akan in Electrical and Electronics Engineering from Koc University, Istanbul, Turkey in 2013. At the same time, he was a research assistant in the Next-generation and Wireless Communications Laboratory (NWCL), Koc University. His current research interests include cognitive radio sensor networks, and network coding.